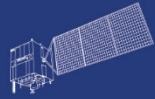


HY



HJ-1AB



CBERS



Gaofen



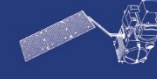
Beijing-2



Sentinel-1



Sentinel-2



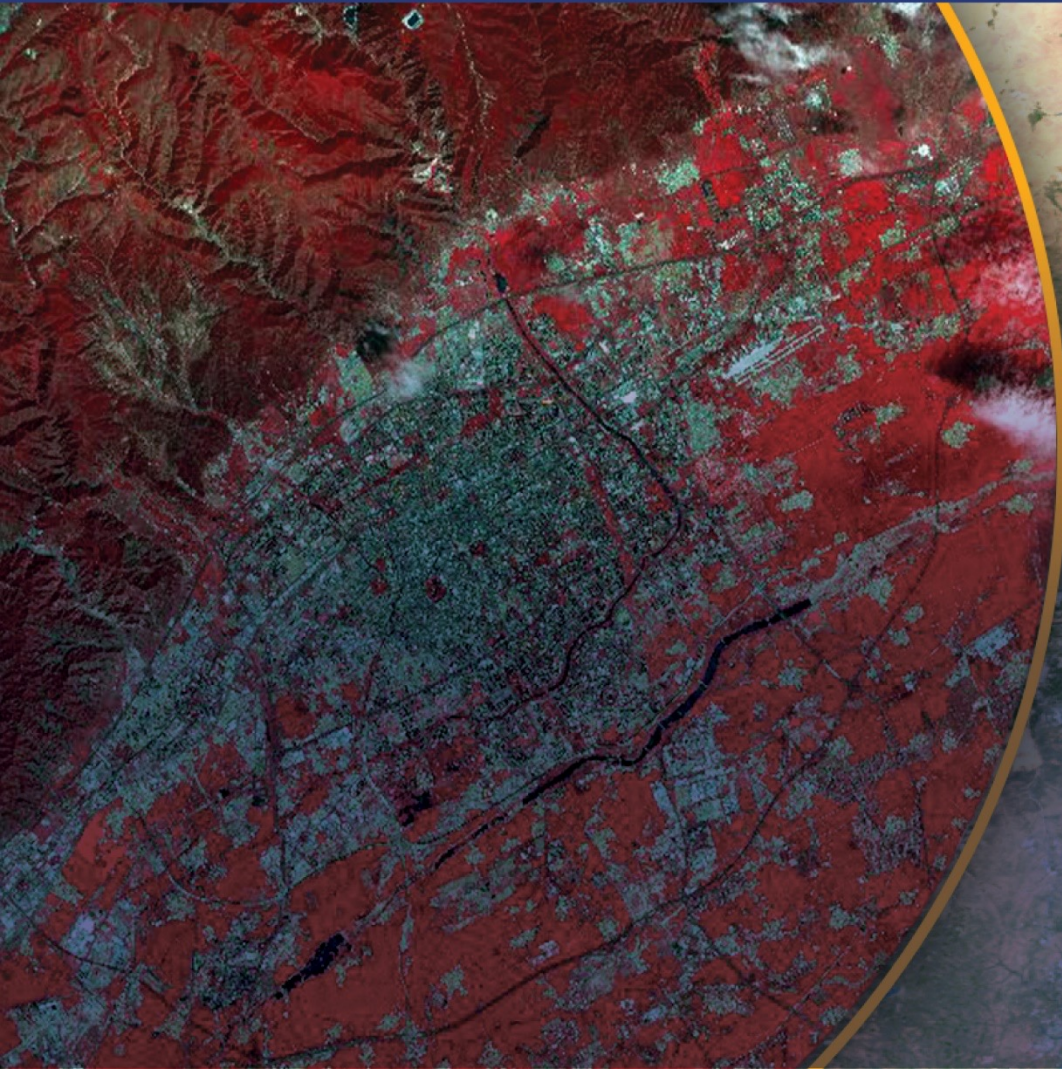
Sentinel-3



Sentinel-5p



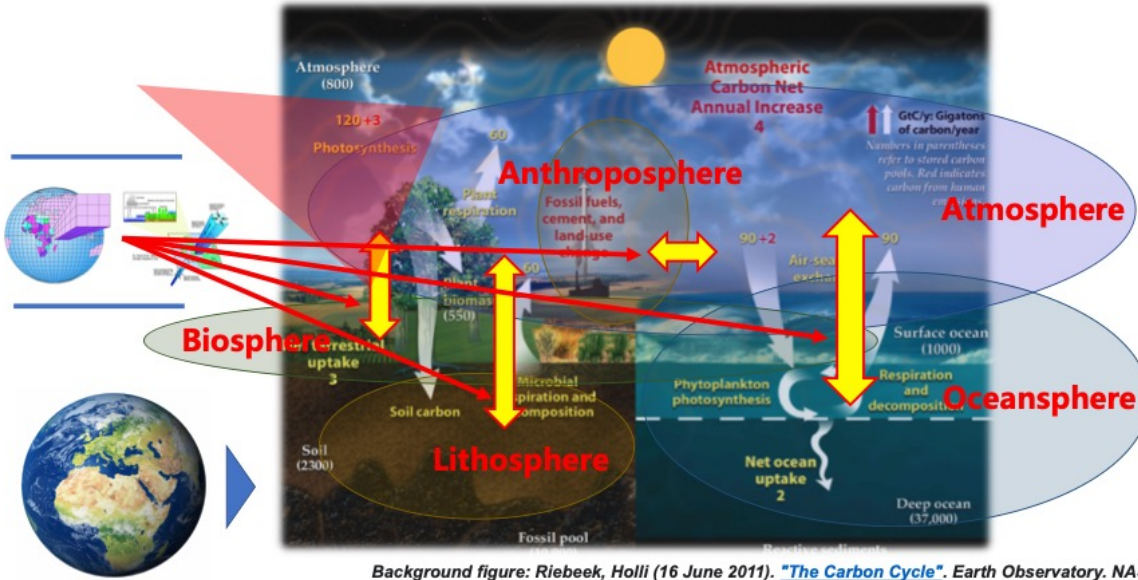
Aeolus



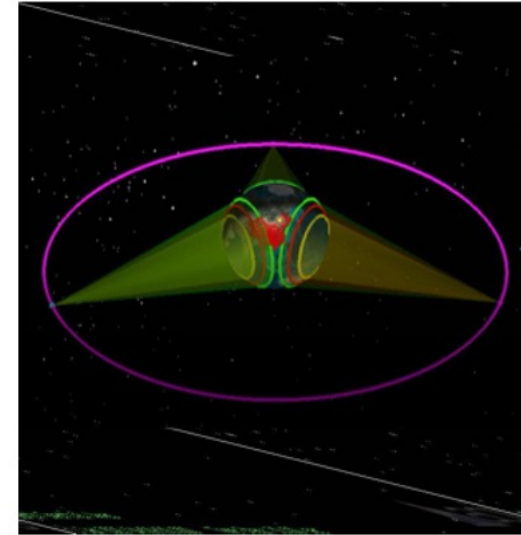
Monitoring ghg from space: TanSat-2 city monitoring and validation

Yi Liu, Dongxu Yang et al.

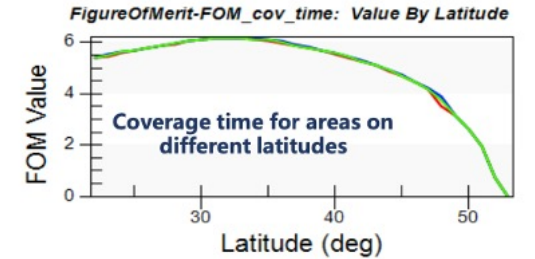
1. TanSat-2 city monitoring simulation
2. GHGs surface measurement and Validation



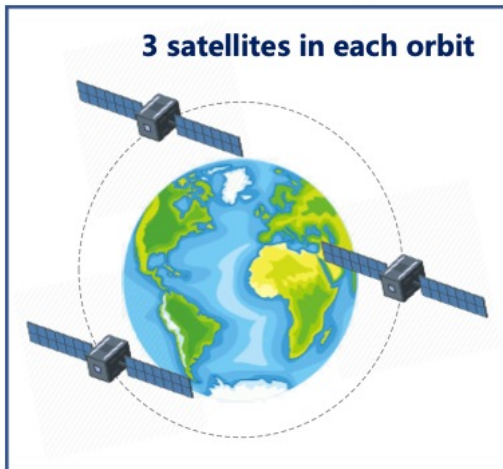
Background figure: Riebeek, Holli (16 June 2011). "The Carbon Cycle". Earth Observatory. NASA



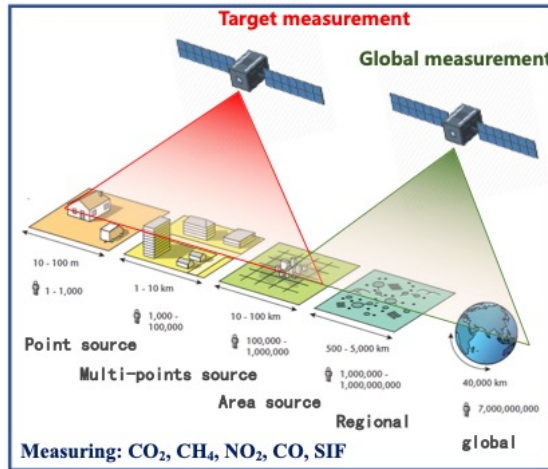
MEO satellites option advantages in global coverage and revisit period



LEO satellites option

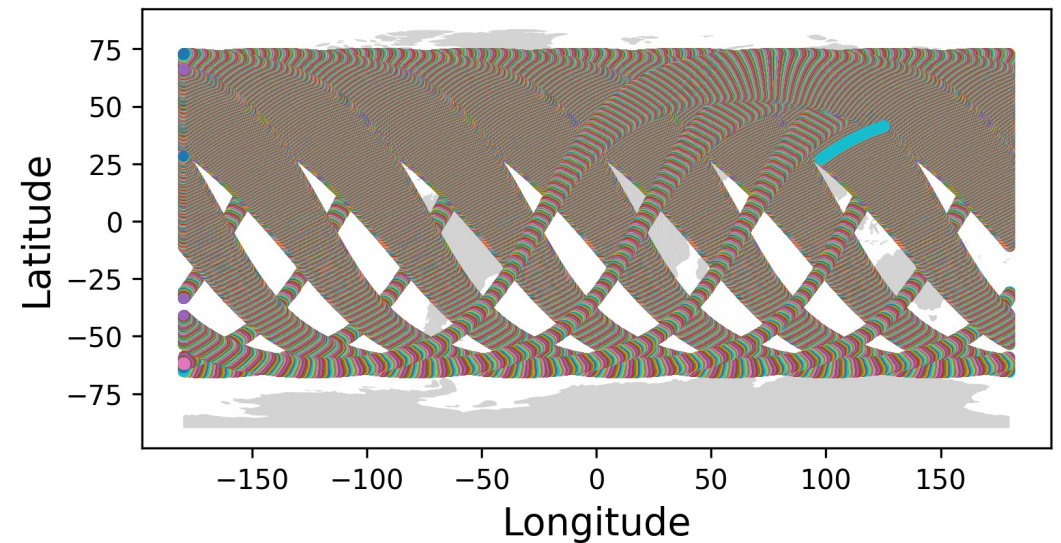
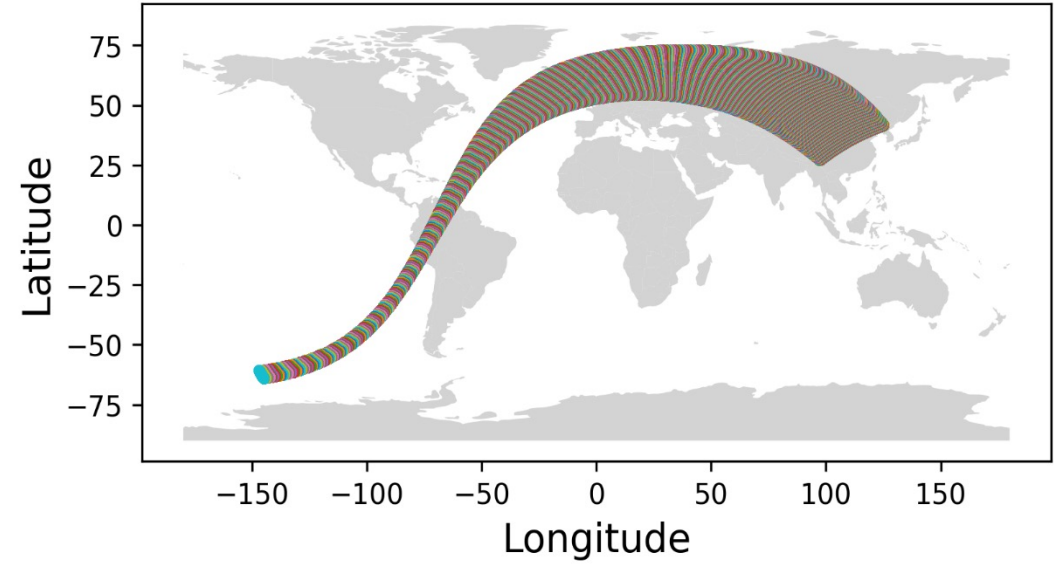
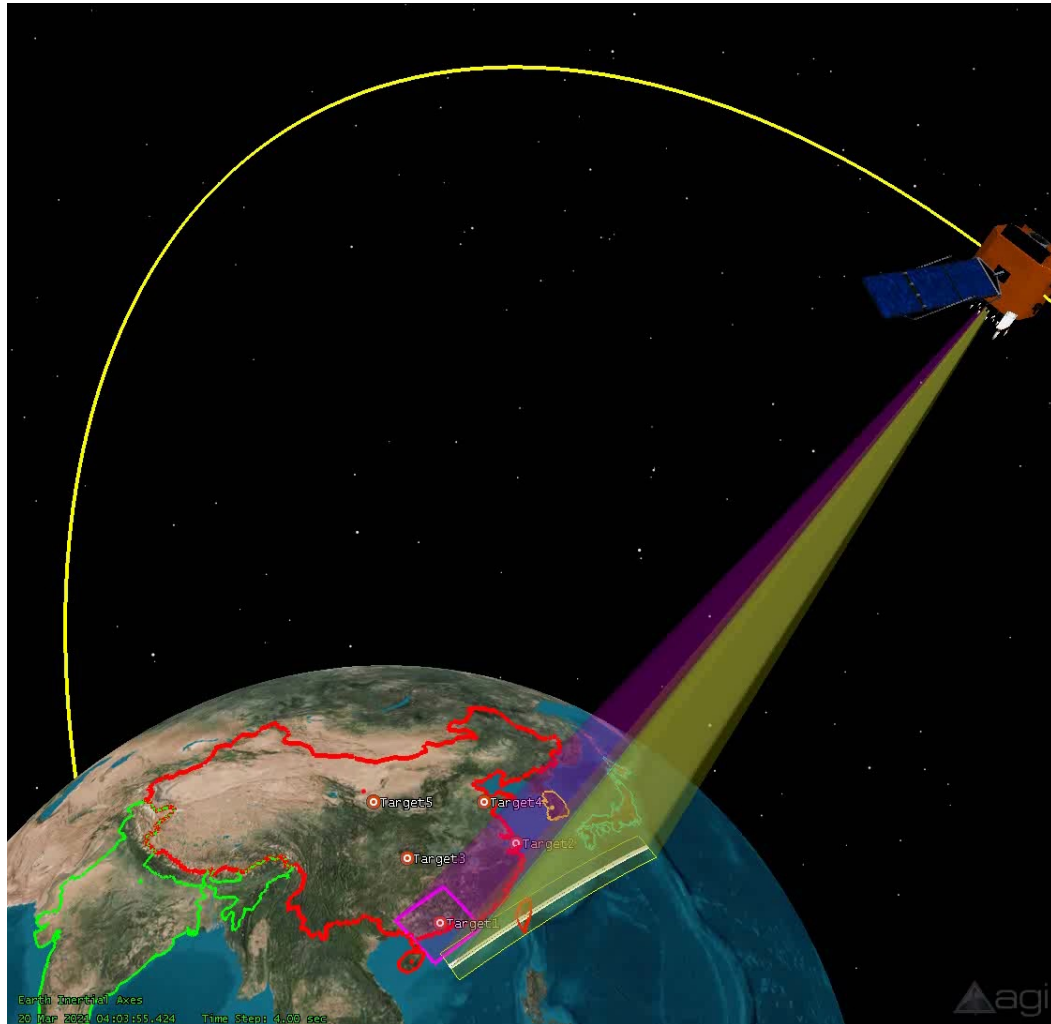


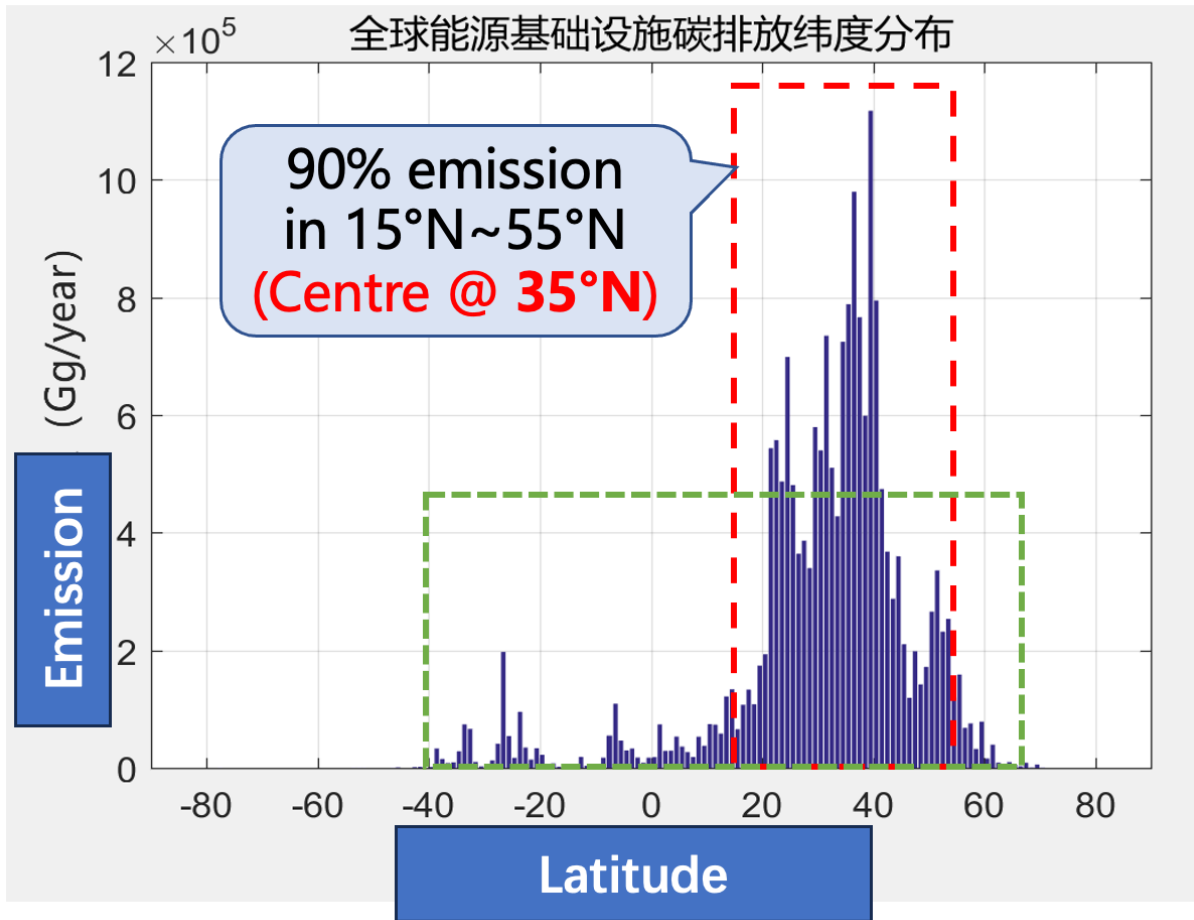
Multiple satellites



- **XCO₂: 1 ppm precision**
- **XCH₄: 8 ppb precision**

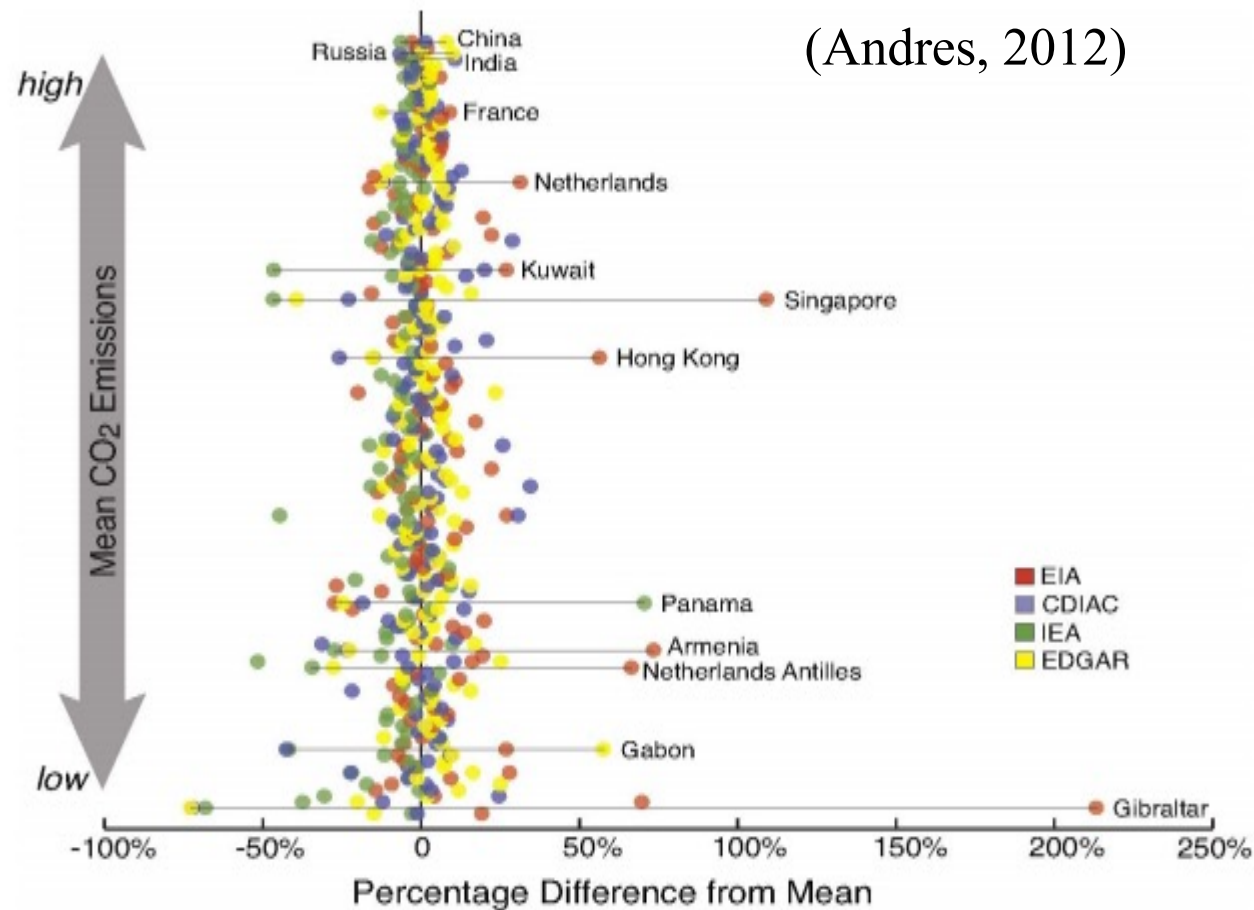
Bands	NO ₂ Band	O ₂ A Band	Weak CO ₂	Strong CO ₂	CH ₄ Band
Geophysical P.	NO ₂	O ₂ , SIF	CO ₂ , CH ₄	CO ₂	CH ₄ , CO
Range /μm	0.4-0.49	0.747-0.773	1.590-1.675	1.990-2.095	2.305-2.385
Width /nm	90	26	85	105	80
SR /nm	0.6	0.12	0.3	0.35	0.25
SSI	3	3	3	3	3
TanSat SNR@Lref (photons/s/nm/cm2/sr)	800@2.4E13	620@6.4E12	520@2.1E12	480@1.8E12	150@8.5E11
CO ₂ @Lref (photons/s/nm/cm2/sr)	500@1.3E13	330@6.4E12	400@2.1E12	400@1.8E12	





Orbit characters	Value
Perigee	522km
Apogee	7840km
Inclination	116.565°
Lat @ Apogee	35°N
repeat cycle	1day
delta Resolution	0.87km
Swath	2900km
OZA	<30°

Inventory: small-scale flux estimates are aggregated together to form a total emission inventory using activity data (energy consumption, population density, traffic data and local air pollution reporting) and simulation tools



Inventories are prone to **systematic errors** and their **uncertainties** are not well known

Seasonality of ODIAC CO₂ff emissions in Beijing

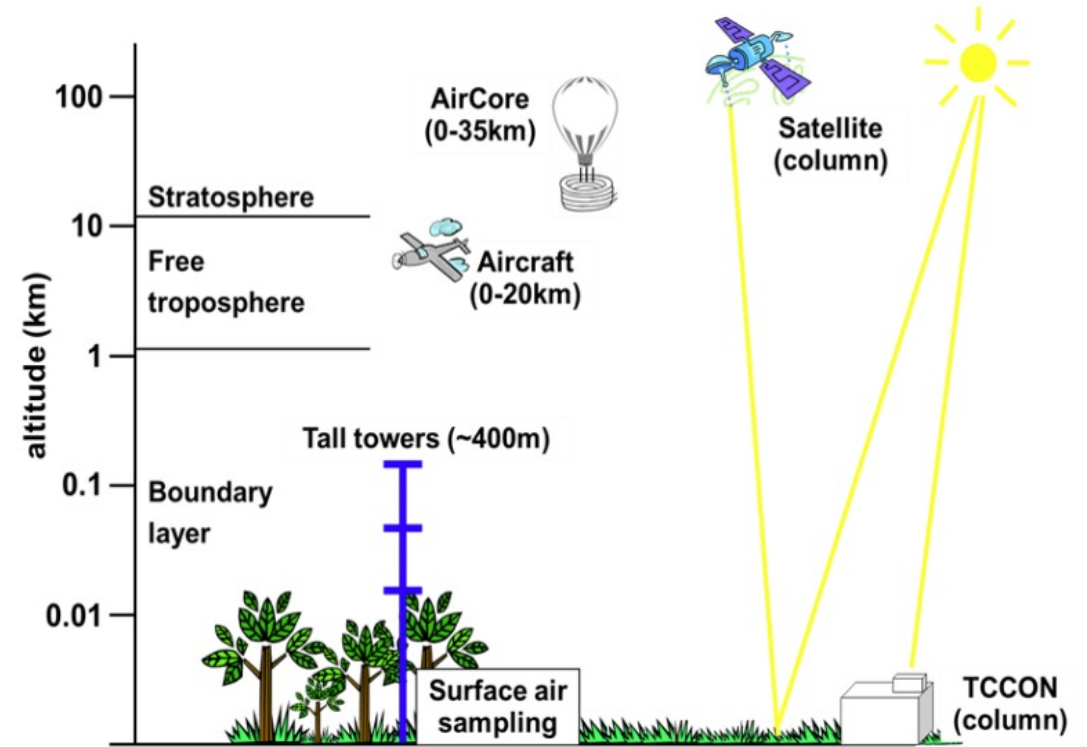
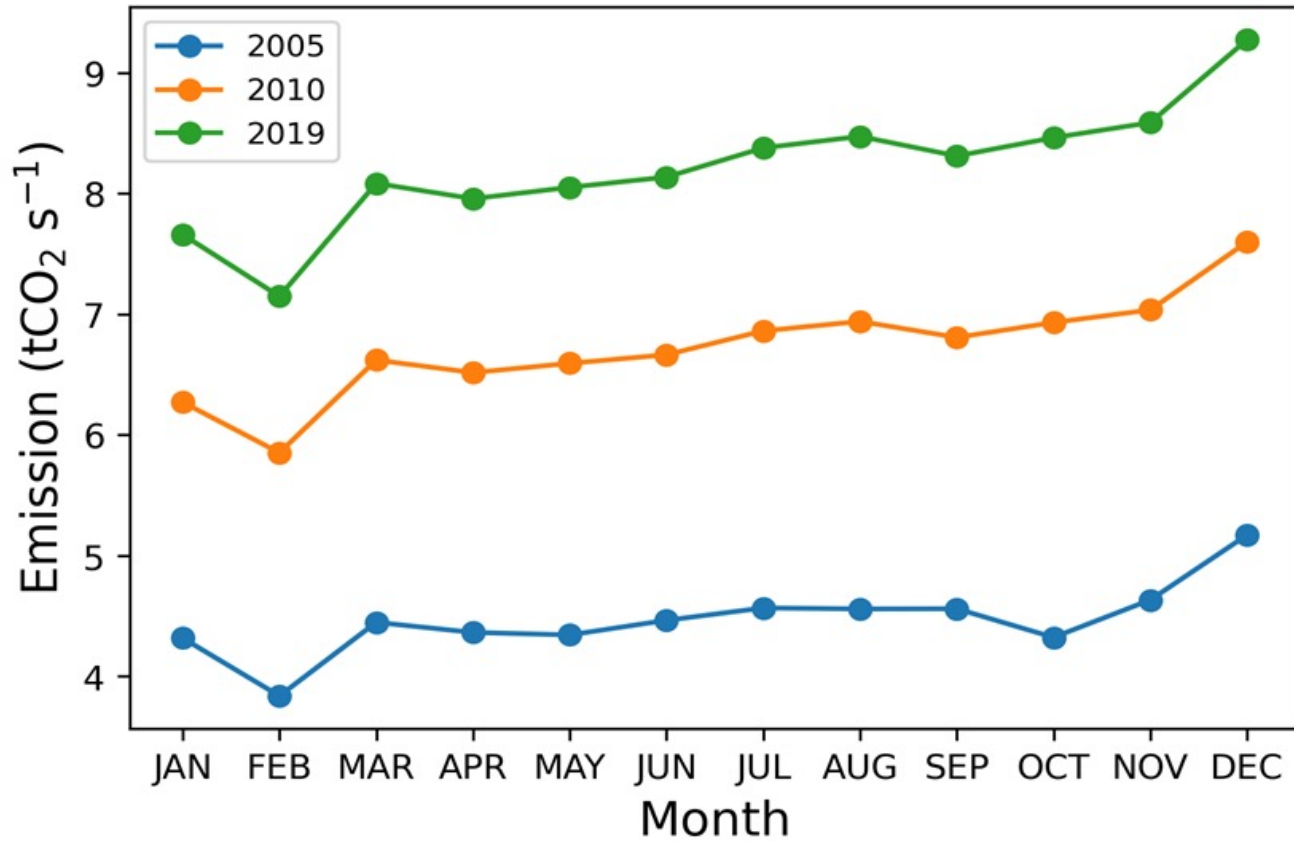


Figure 1: Observations of atmospheric greenhouse gases

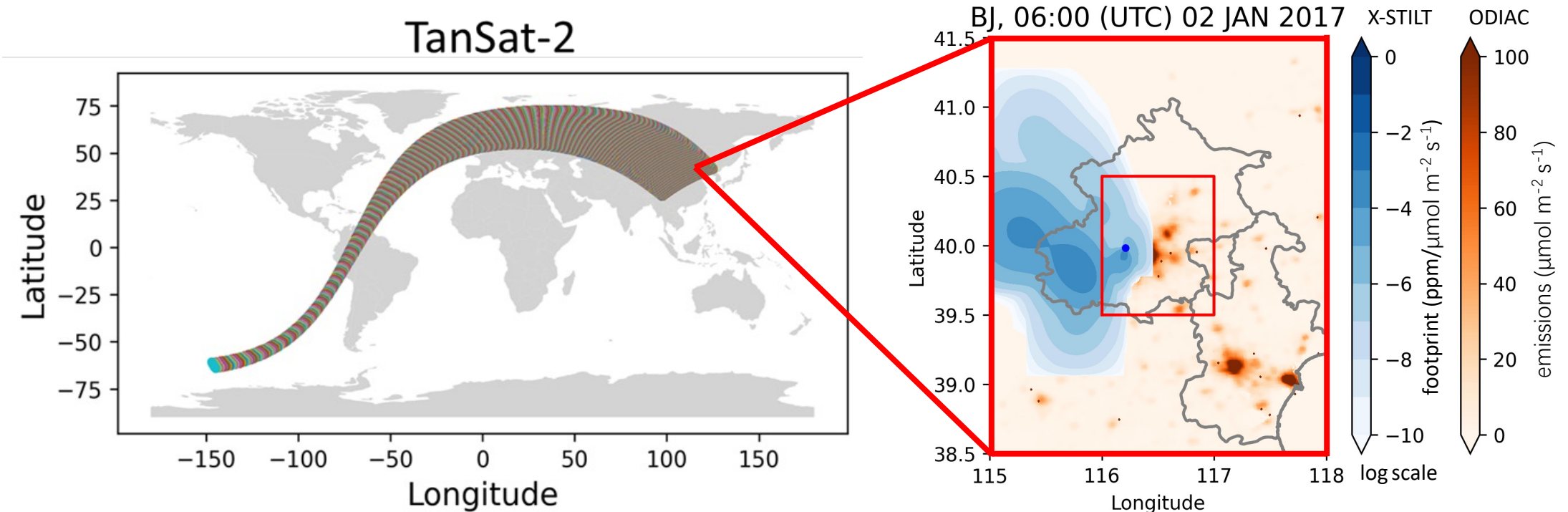
Image courtesy of the ICOS report

- Limited ability of inventory for assessing the seasonality of anthropogenic CO₂ emissions
- Atmospheric CO₂ measurements are valuable to verify emissions inventories

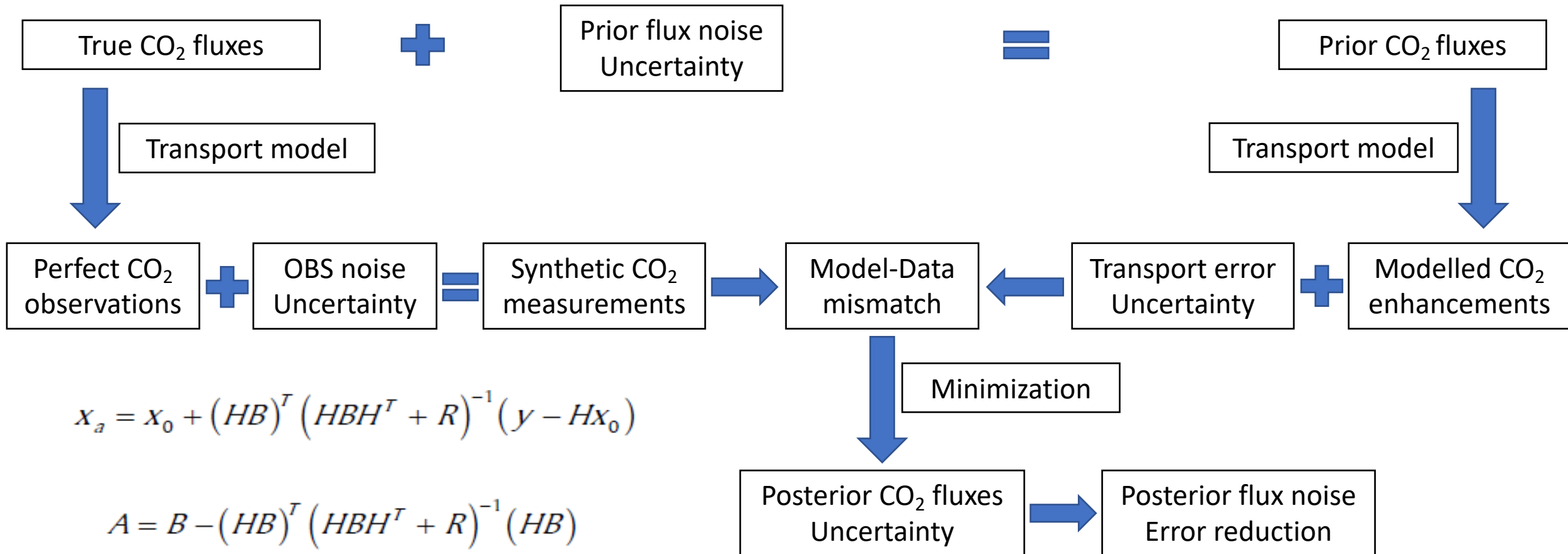
TanSat-2 is planned to be launched in 2025 to measure column-averaged CO₂ (XCO₂) at 3000 km wide across-track swaths, with a pixel size of 2 km × 2 km.

The precision of satellite sampling is expected to be less than 1 ppm.

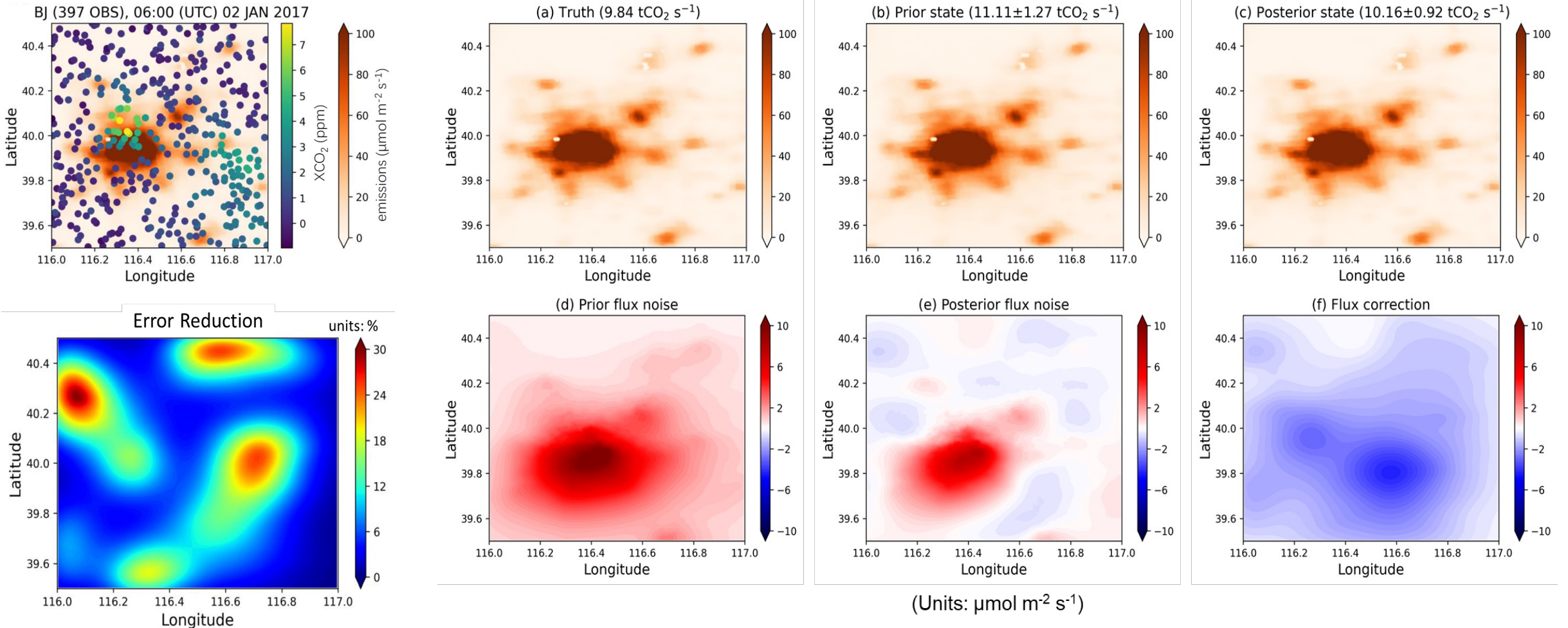
X-STILT and ODIAC at 1 km resolution are used to simulate synthetic data and develop an urban CO₂ inversion system.



To **minimize** the mismatch between observed and modeled [CO₂] by **optimizing** the prior fluxes



- ERA5 total cloud cover data are used to identify cloud-free samples of TanSat-2.
- Outside the growing season, assimilating cloud-free TanSat-2 data can have a 20-30% reduction in prior flux errors.



- Test the impacts of sampling patterns and XCO₂ retrieval errors on reducing prior flux errors.
- Correction in systematic flux errors is sizable, subject to unbiased satellite sampling and favorable meteorological conditions (less cloud cover and low wind speed).

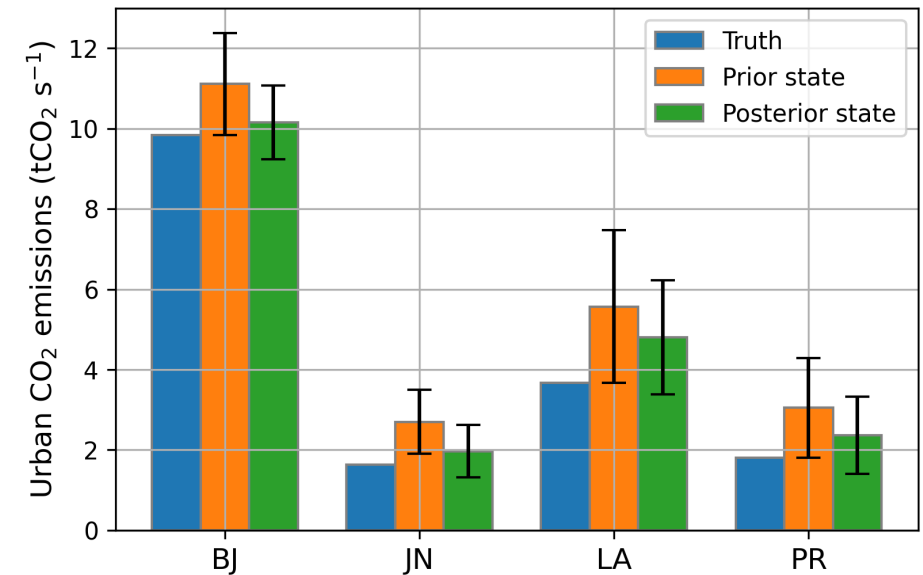
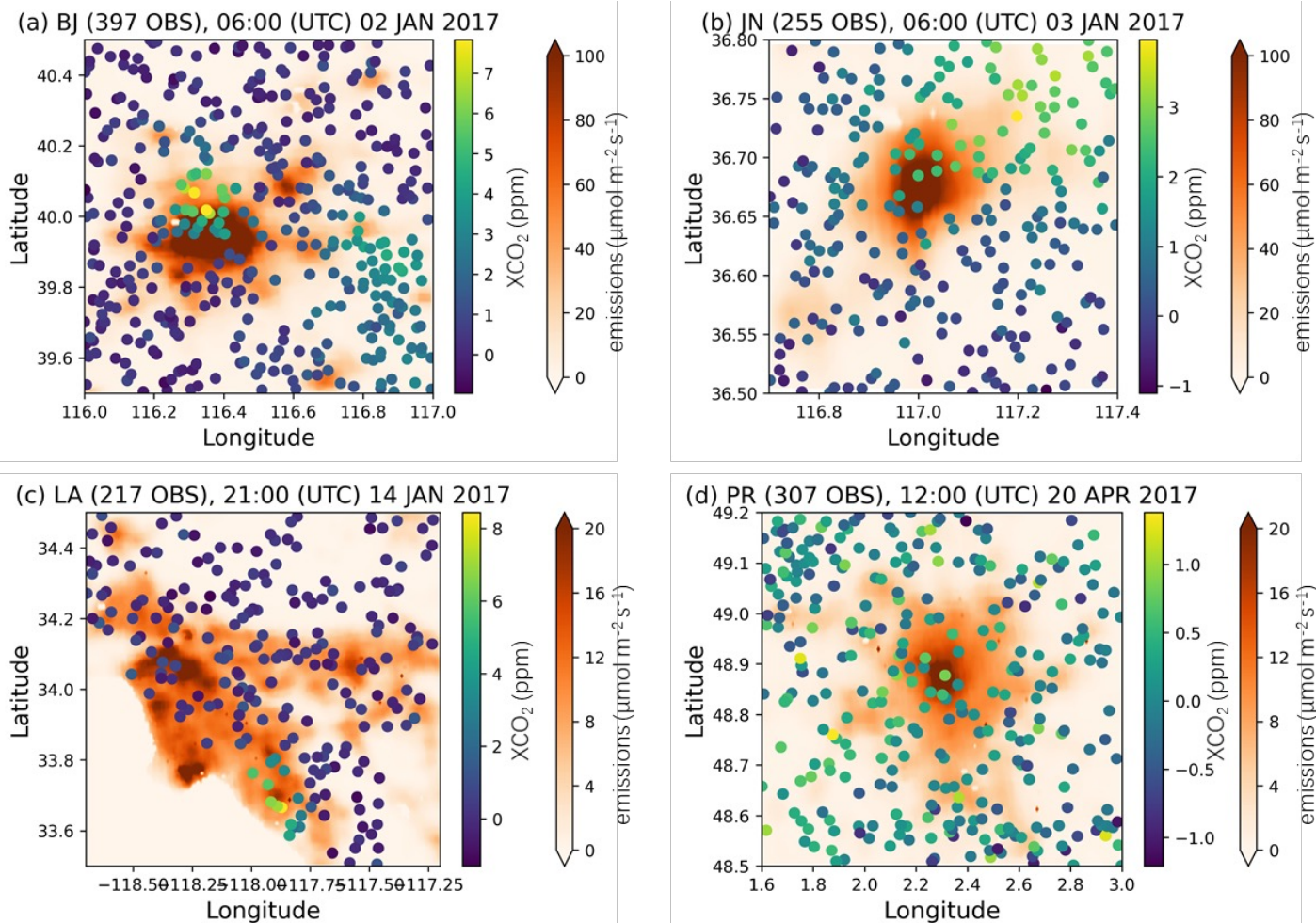


Table 1. Reduction of flux bias and random error (RE) and overall correction (OC) of integrated urban CO₂ emissions in Beijing (BJ), Jinan (JN), Los Angeles (LA), and Paris (PR). Units are %.

City	Bias	RE	OC
BJ	75	28	46
JN	68	19	45
LA	40	25	32
PR	56	23	37

- Reduction in systematic and random flux errors is correlated with the signal-to-noise ratio of satellite measurements, which is 2.8 (BJ), 2.1 (JN), 0.7 (LA), and 0.1 (PR), related to different magnitudes of error reduction.

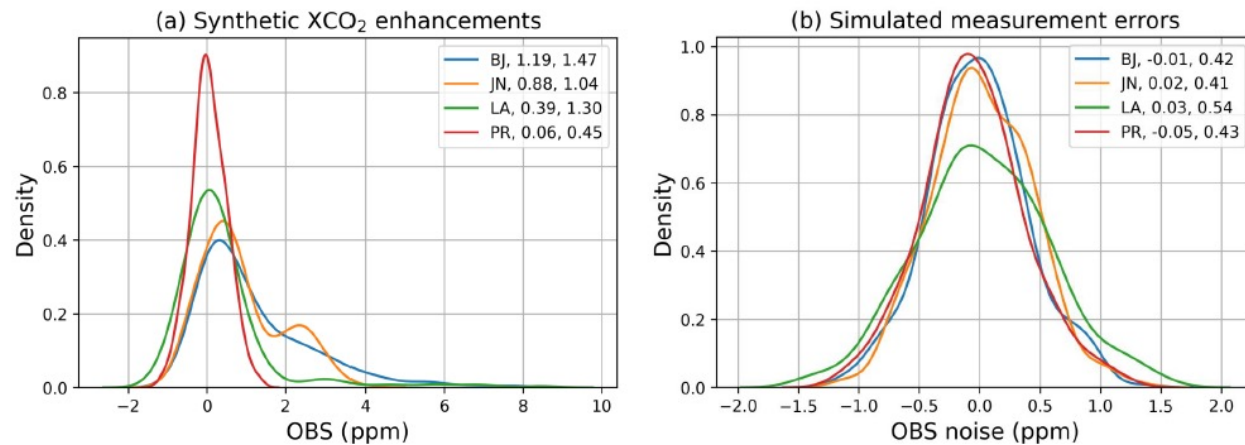


Figure 4. Probability density of synthetic X_{CO₂} enhancements over Beijing (BJ), Jinan (JN), Los Angeles (LA), and Paris (PR) (a) and the corresponding measurement errors (b). The values after the city name are the mean (first number) and standard deviation (second number), and units are ppm.

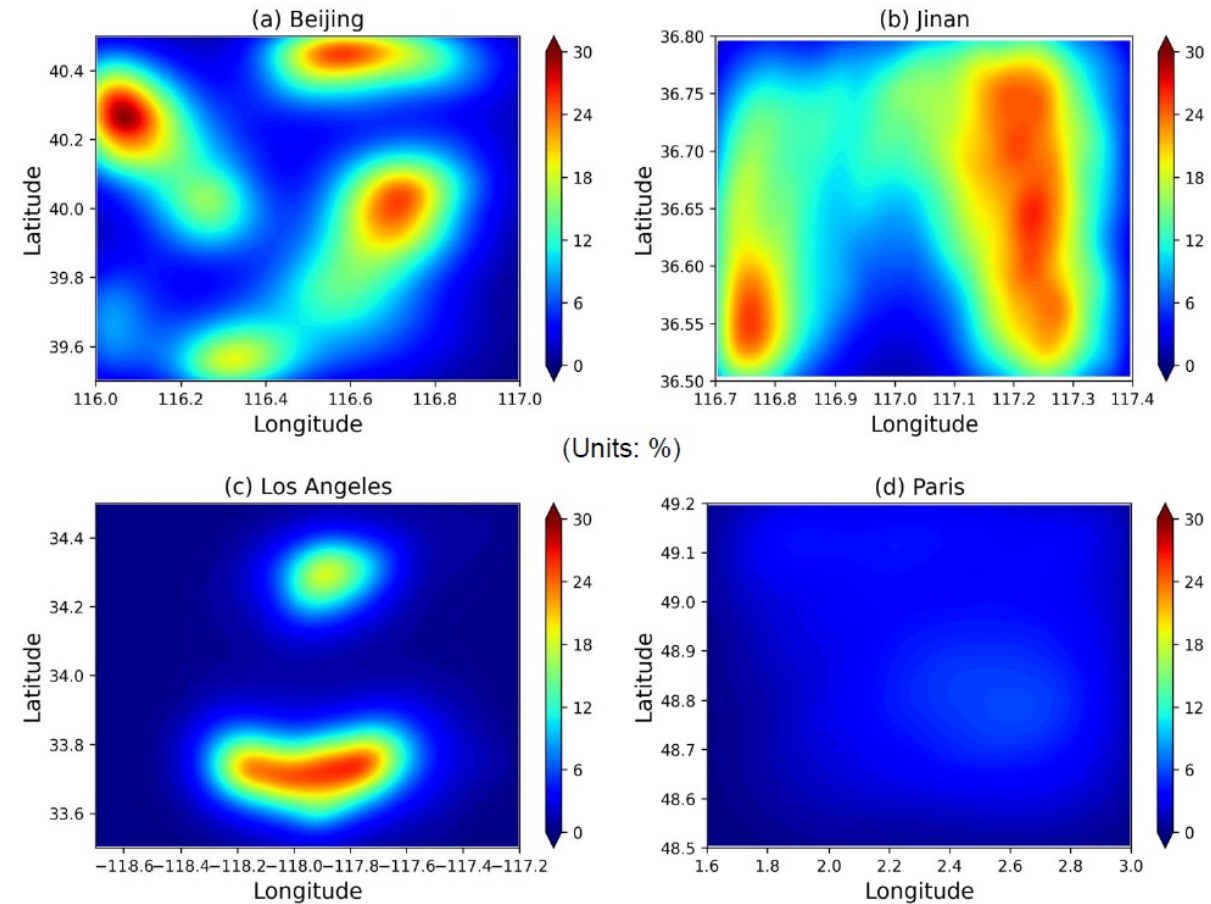


Figure 5. Flux error reduction in Beijing (a), Jinan (b), Los Angeles (c), and Paris (d).

- A systematic measurement error of 1 ppm would significantly degrade emission estimates inferred from satellite data
- The scenario of 4 km resolution (127 OBS) with 1 ppm uncertainty has similar error reduction to the scenario of 8 km (76 OBS) with 0.75 ppm random error, indicating better measurement precision can partially compensate for lower observation density.

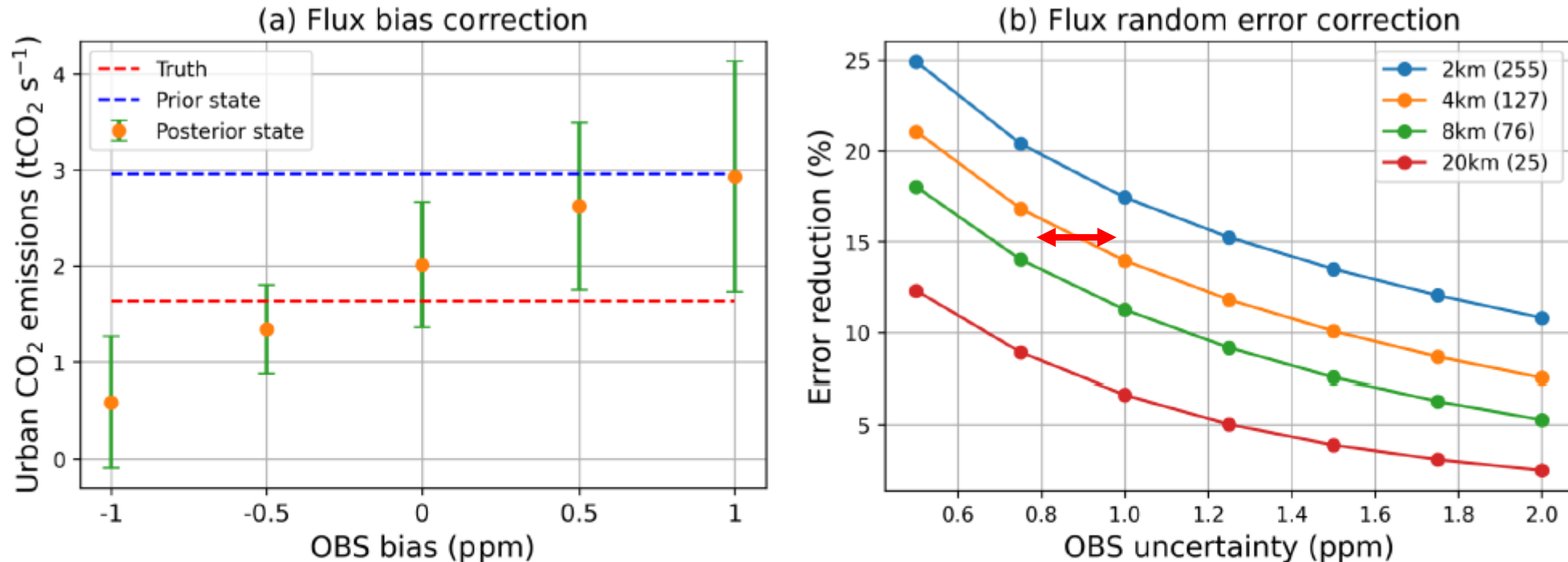
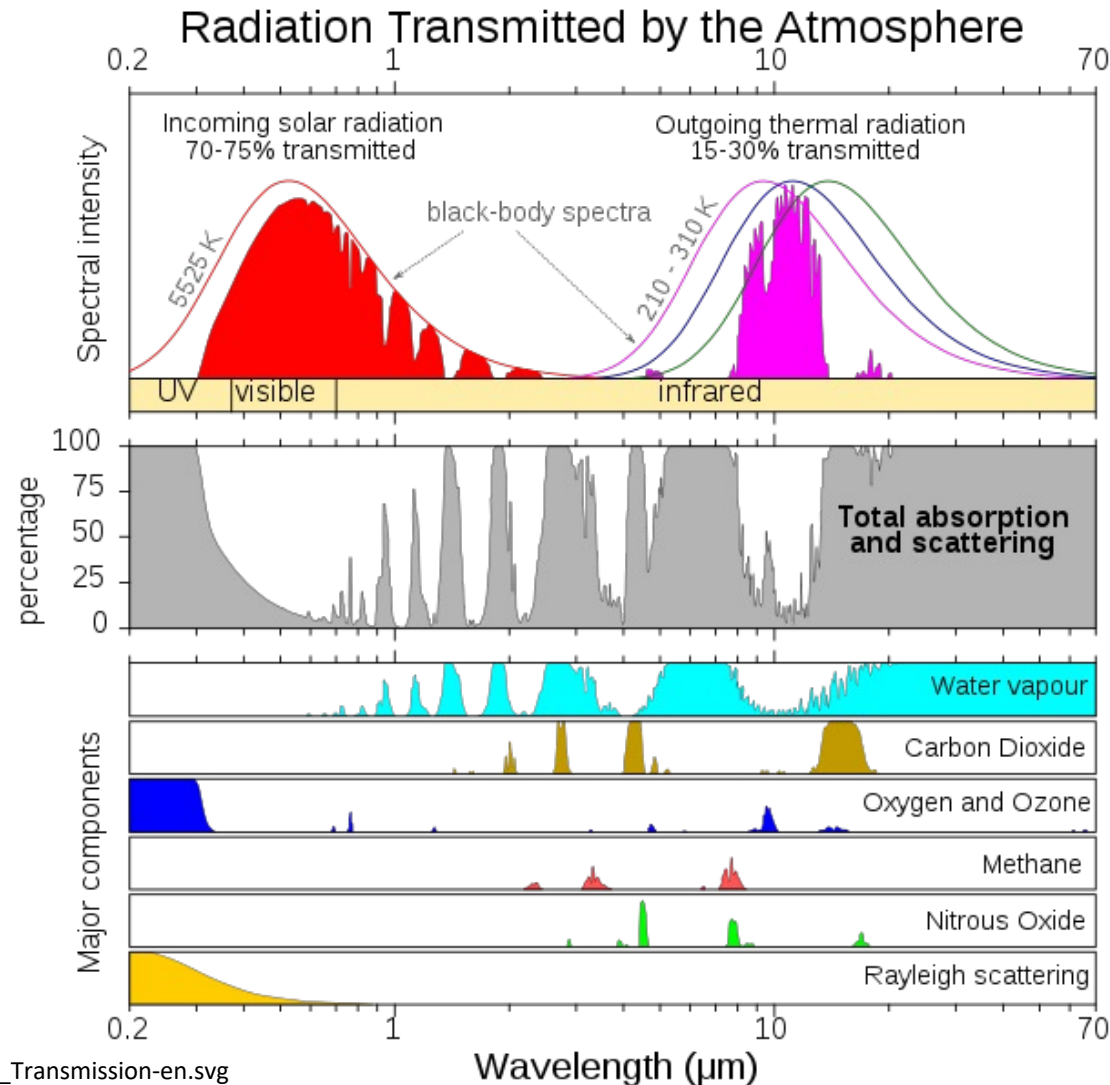
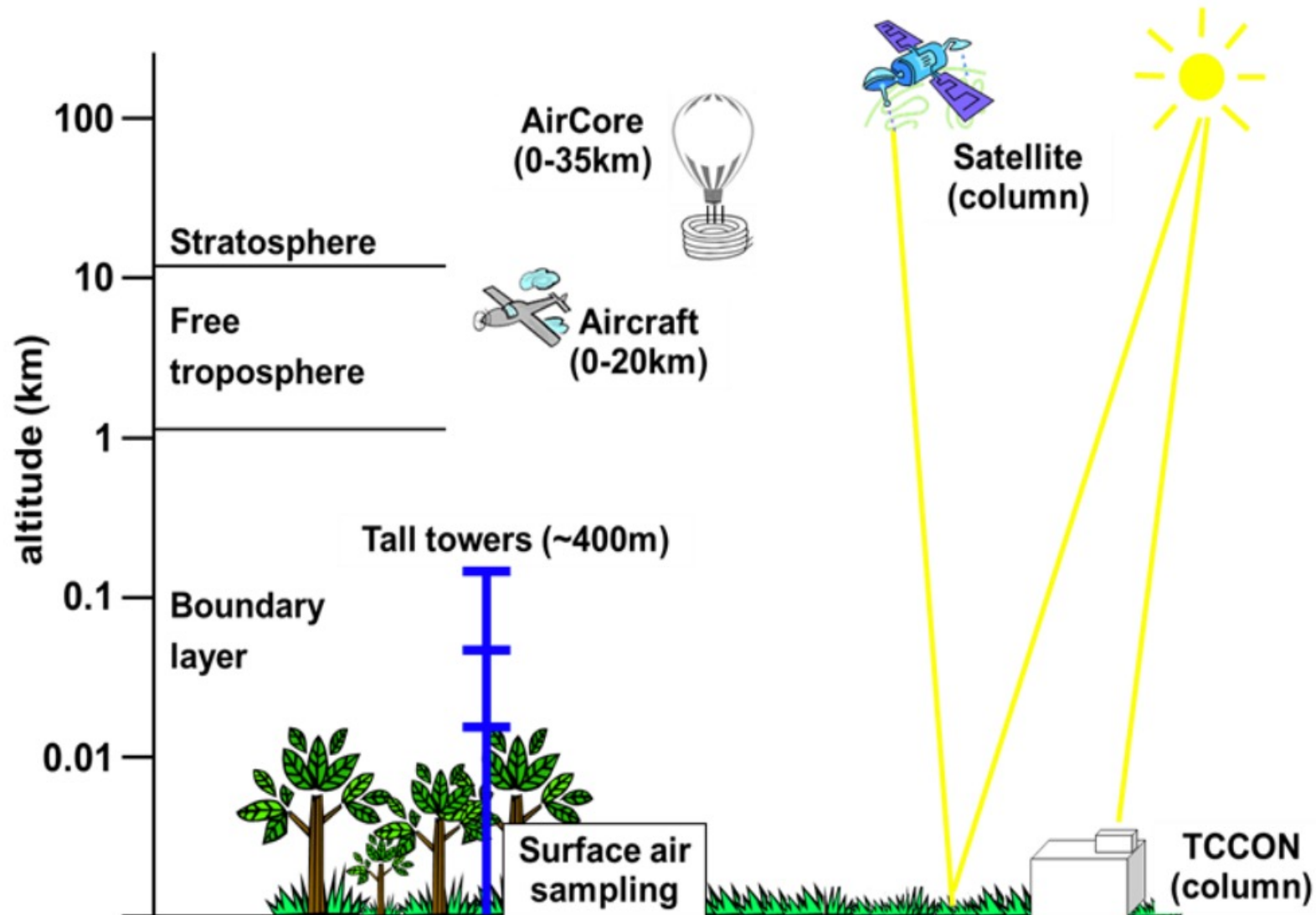


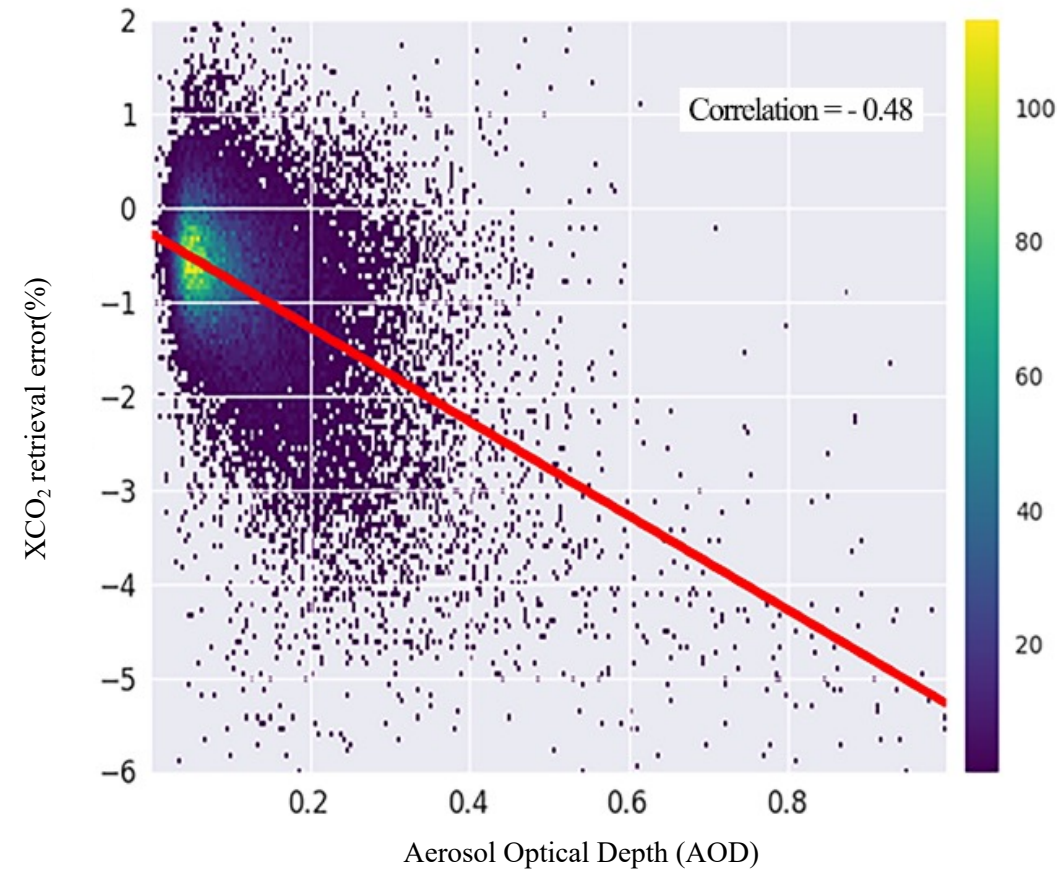
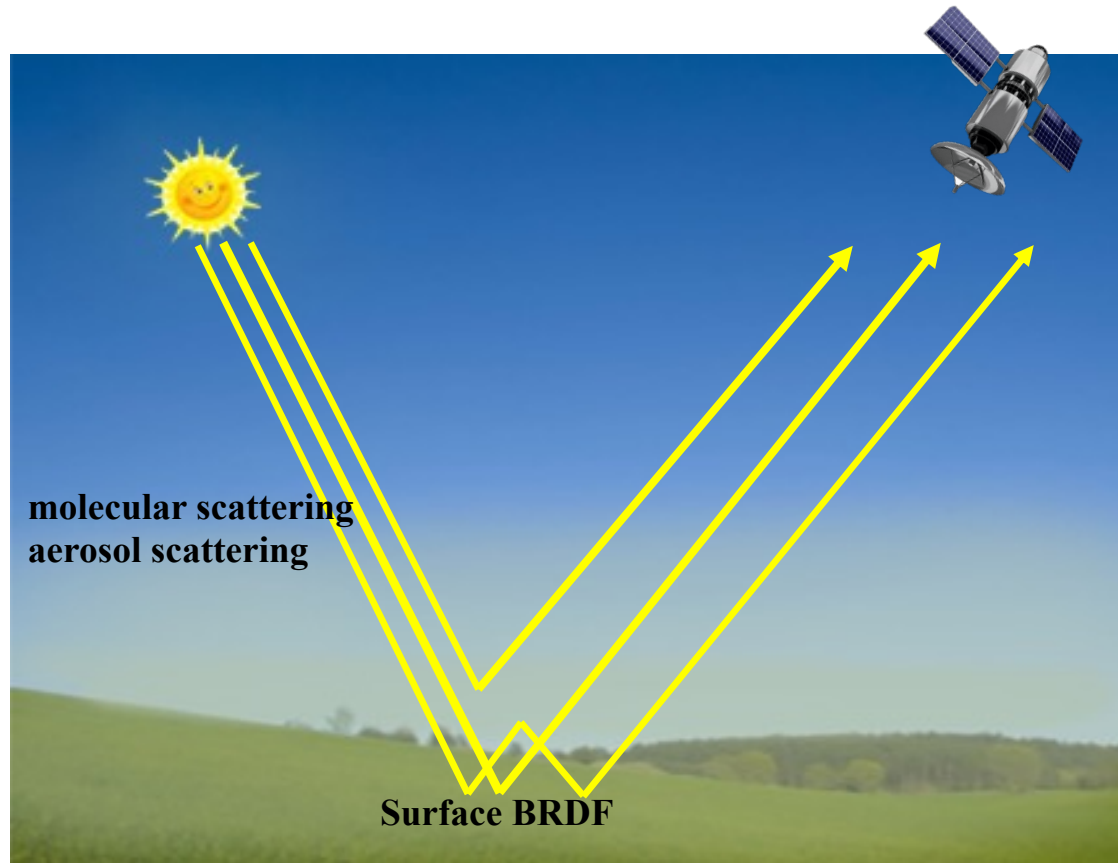
Figure 8. Correction of flux bias with the change of observation bias in Jinan (a) and reduction of spatially-averaged random flux error with the change of observation uncertainty under different sampling resolutions in Jinan (b). The numbers in parentheses are the number of observations.

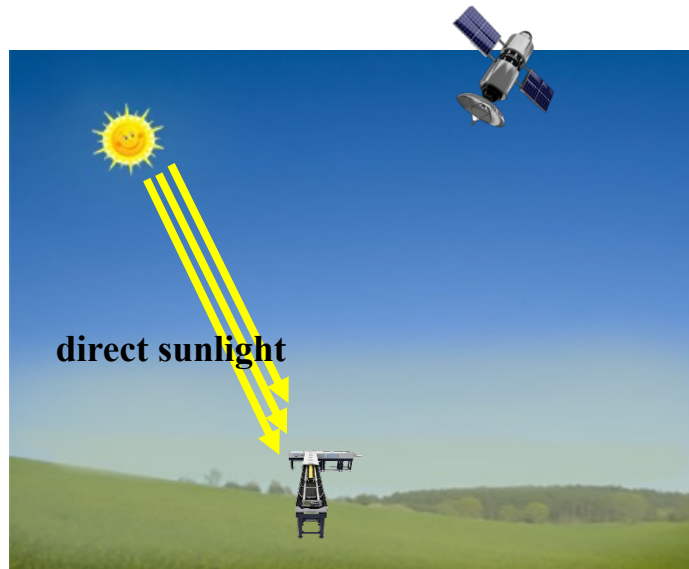
1. TanSat-2 city monitoring simulation
2. GHGs surface measurement and Validation

➤ Greenhouse gases(GHG) (CO_2 , CH_4 , N_2O , CFC...)









GES DISC Data Collections - oco-2

Atmospheric Composition, Water & Energy Cycles and Climate Variability

Data Collections Showing 1 - 25 of 78 datasets associated with oco-2

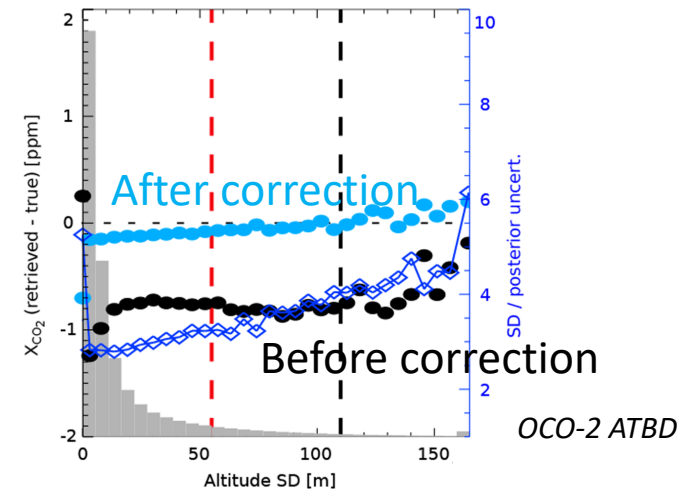
Refine By

- Features
 - Cloud Enabled (4)
- Subject
 - Atmospheric Chemistry (70)
 - Infrared Wavelengths (16)
 - Platform Characteristics (8)
 - Vegetation (2)
- Measurement
 - Atmospheric Carbon Dioxide (68)
 - Attitude Characteristics (4)
 - Carbon Dioxide (2)
 - Infrared Radiance (16)
 - Orbital Characteristics (4)

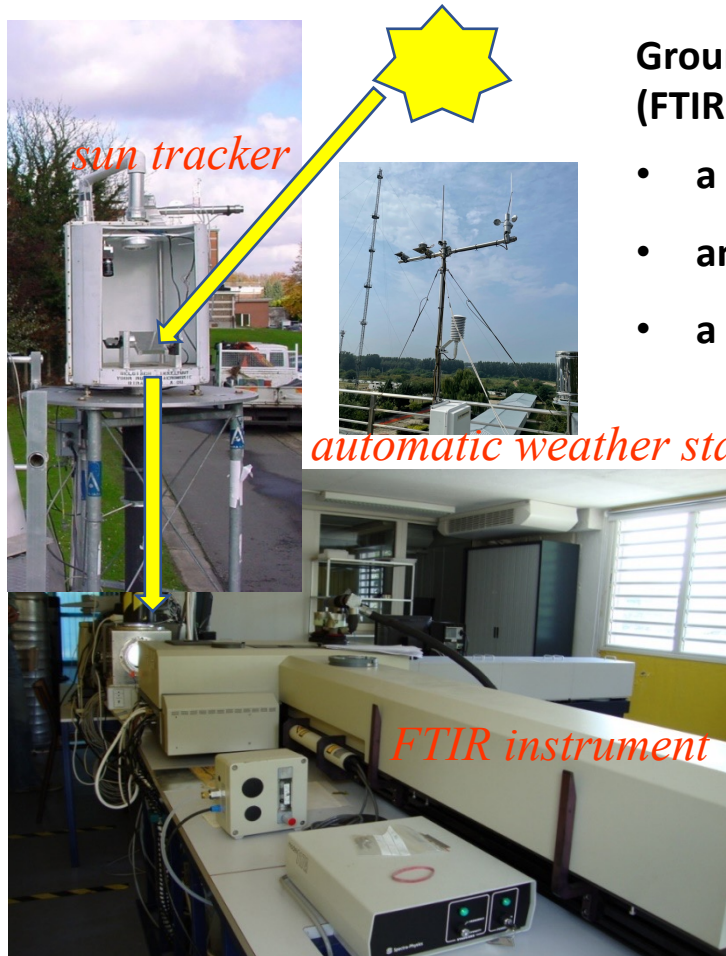
Dataset

Dataset	Source	Version	Time Res.	Spatial Res.	Process Level	Begin Date	End Date
OCO-2 Level 2 bias-corrected XCO ₂ and other select fields from the full physics retrieval aggregated as daily files, Retrospective processing V11r (OCO2_L2_Lite_FP 11r)	OCO-2 OCO-2	11r	16 days	2.25 km x 1.29 km	2	2018-11-01	2022-10-02
OCO-2 Level 2 bias-corrected soil-induced fluorescence and other select fields from the IMAP-DOAS algorithm aggregated as daily files, Retrospective processing V11r (OCO2_L2_Lite_SIF 11r)	OCO-2 OCO-2	11r	16 days	2.25 km x 1.29 km	2	2018-12-01	2022-10-01

Corrected products

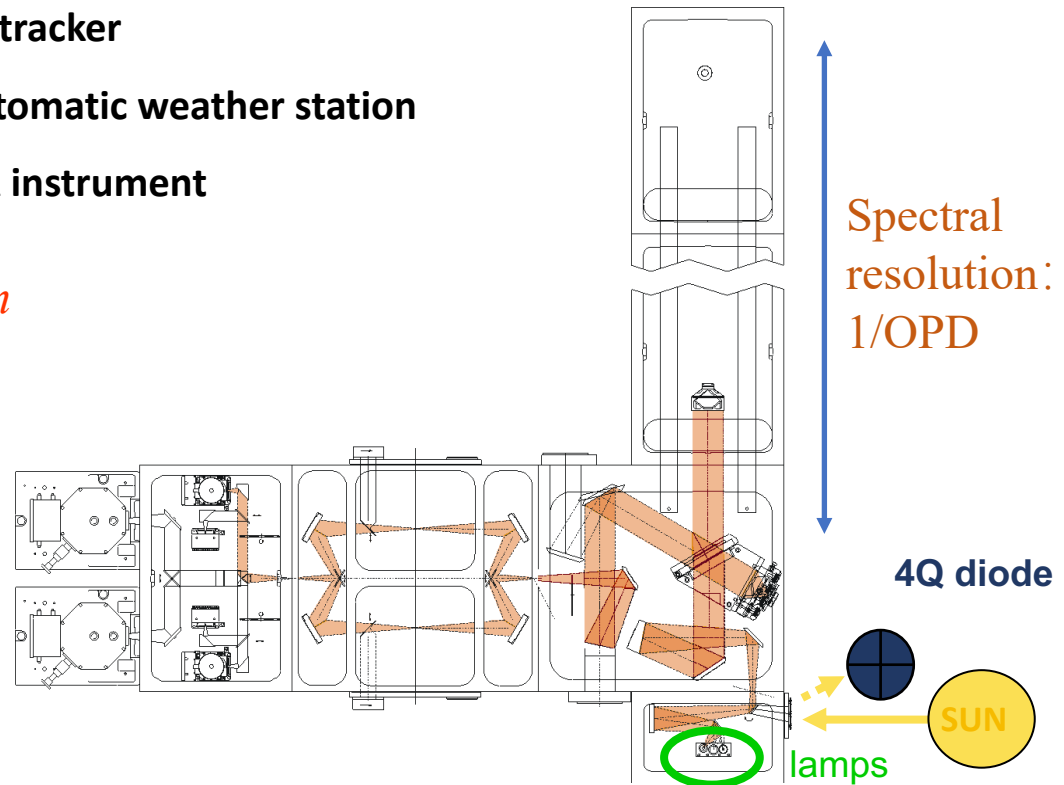


record direct solar radiation, the spectral resolution can up to $0.003\text{-}0.5\text{ cm}^{-1}$
 principle: Michelson Interference



Ground-based Fourier-transform infrared (FTIR) measurement system

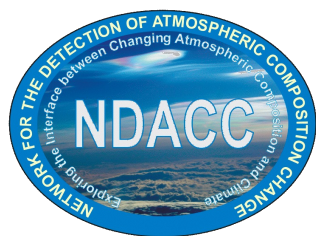
- a sun tracker
- an automatic weather station
- a FTIR instrument



Detection of Atmospheric Composition Change – the Infrared Working Group

NDACC IRWG

- mainly Bruker IFS 120HR/125HR
- thermal infrared 800 - 4800 cm^{-1}
- 0.0036 – 0.005 cm^{-1}
- profile/column concentration
- single measurement time ~10 mins



Total Carbon Column Observing Network

TCCON

- Bruker IFS 125HR
- near infrared 4800 - 16000 cm^{-1}
- 0.02 cm^{-1}
- column concentration
- single measurement time - 3 mins

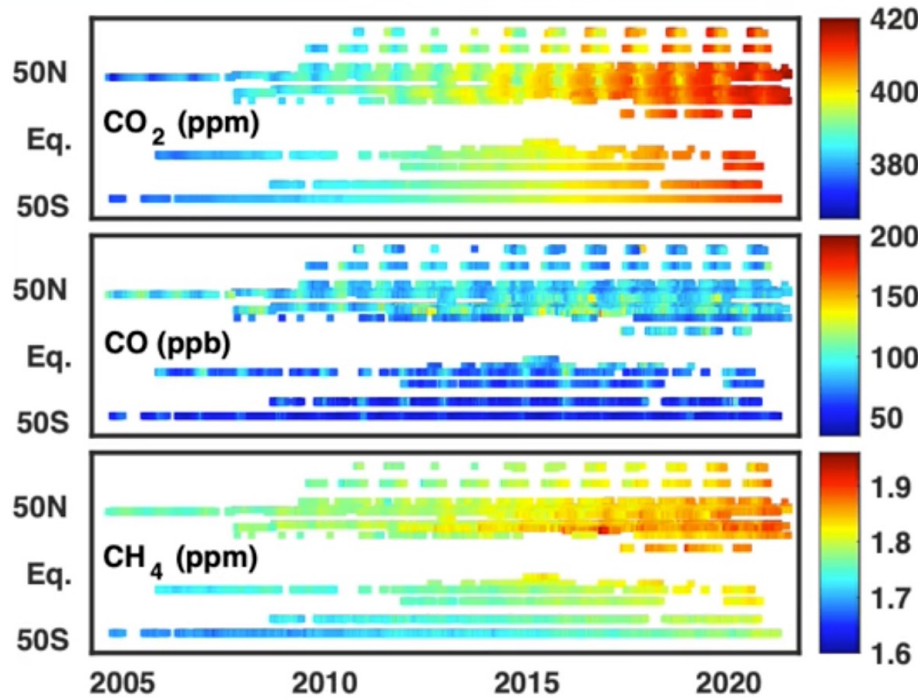


Collaborative Carbon Column Observing Network

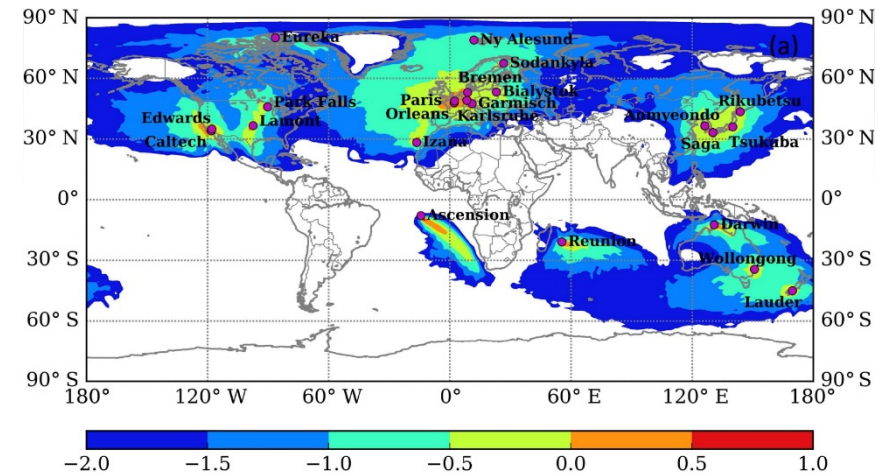
COCCON

- Bruker EM27/SUN
- near infrared 4800 - 12000 cm^{-1}
- 0.5 cm^{-1}
- column concentration
- single measurement time - 1 min





Time series of column-average dry-air mixing ratio of CO₂, CO, and CH₄ based on the TCCON network



Belikov et al., ACP2017

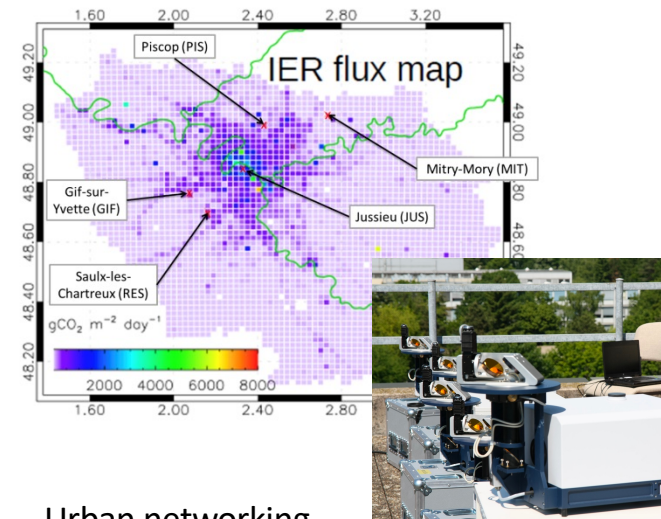
- The concentrations of CO₂, CH₄ increase yearly.
- The concentration of CO shows a decreasing trend.
- Lack of observations in South America, Africa, South-Central Asia (Western China)



Airborne

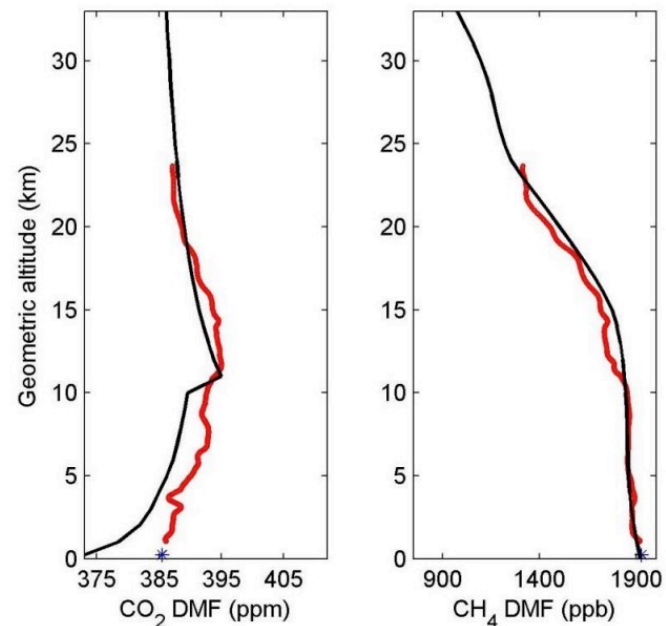
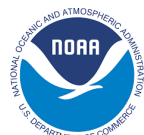
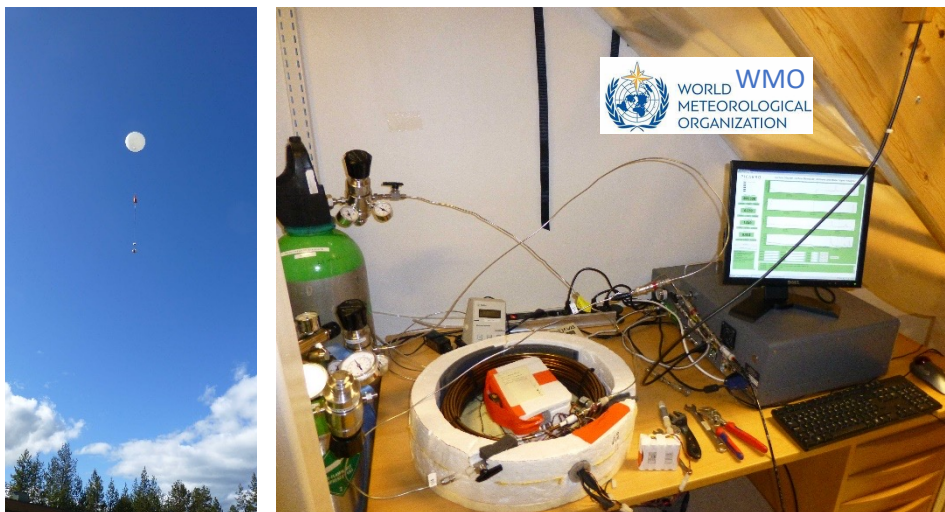


Shipborne

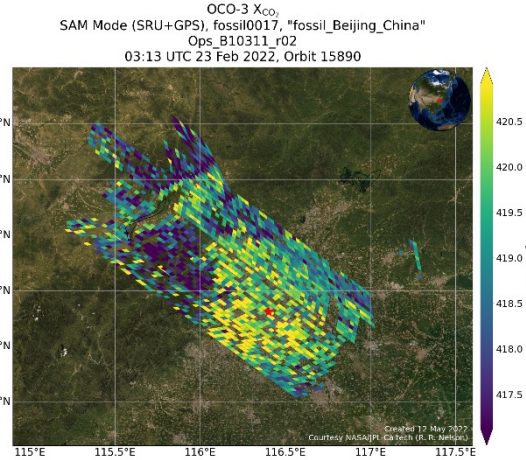


Urban networking observation experiment

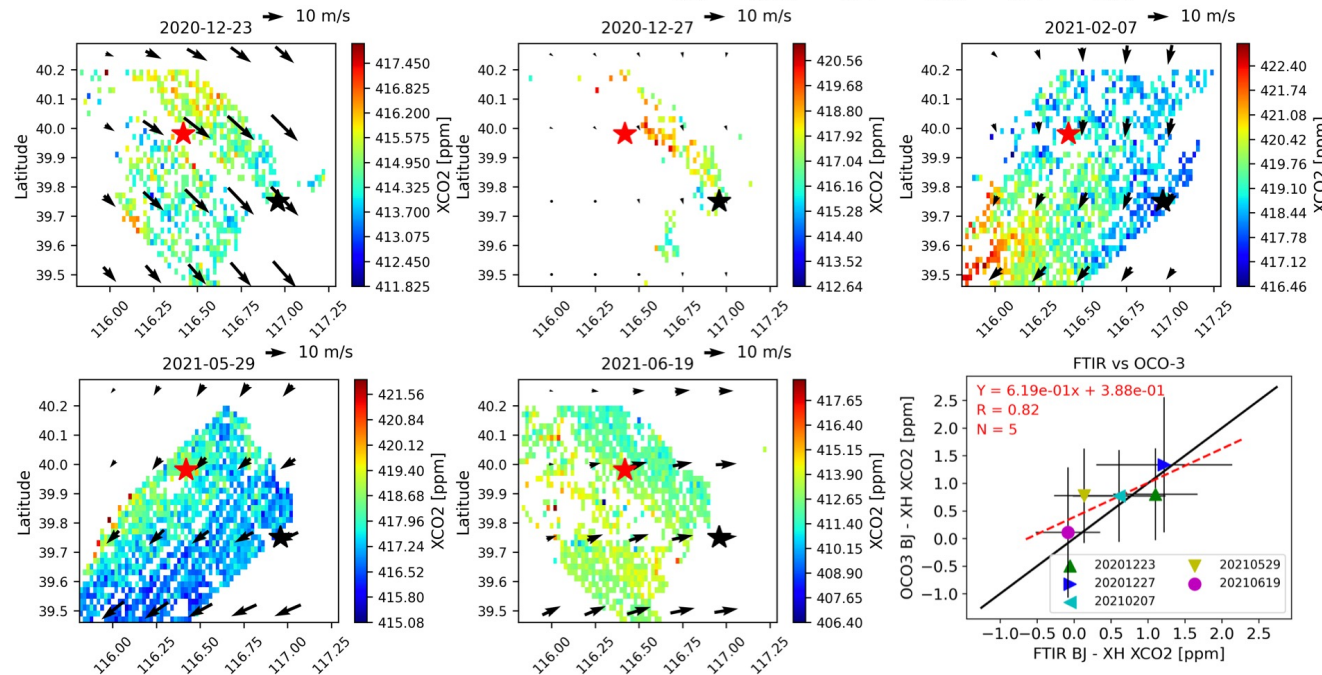
FTIR and AirCore Campaign



red: AirCore measurements
black: TCCON initial values



Two FTIRs (Xianghe and Beijing) are applied to validate the spatial gradient observed by the OCO-3 SAMS XCO₂ measurements (R = 0.82)

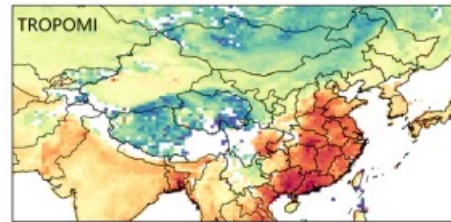


East Asian methane emissions inferred from high-resolution inversions of GOSAT and TROPOMI observations: a comparative and evaluative analysis

Ruosi Liang^{1,2,3}, Yuzhong Zhang^{2,3}, Jingran Liu^{1,2,3}, Wei Chen^{1,2,3}, Peixuan Zhang^{2,3,4}, Cuihong Chen⁵, Huiqin Mao⁵, Guofeng Shen⁶, Zhen Qu⁷, Zichong Chen⁷, Minqiang Zhou⁸, Pucal Wang⁸, Robert J. Parker^{9,10}, Hartmut Boesch^{9,10}, Alba Lorente¹¹, Joannes D. Maasakkers¹¹, and Ilse Aben¹¹

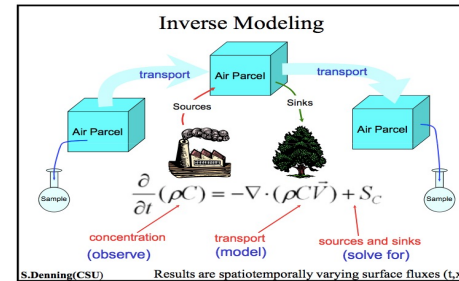
- **The model column concentrations after assimilation with GOSAT are more close to TCCON measurements (Xianghe and Hefei) than TROPOMI.**
- **TROPOMI XCH₄ may still have a bias over China.**

Satellite measurement



assimilation

Model inversion

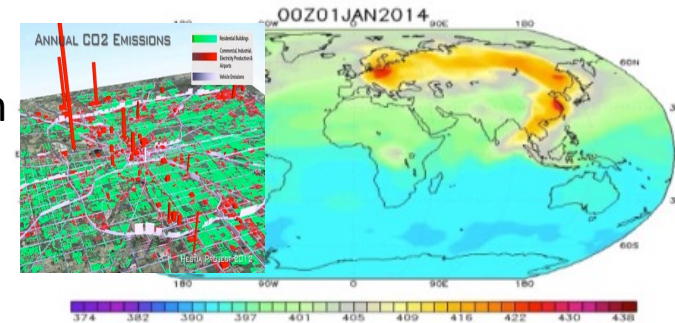


validation



TCCON/COCCON
ground-based measurement

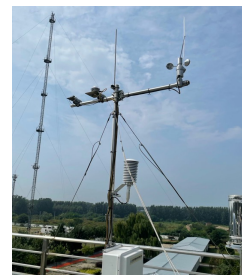
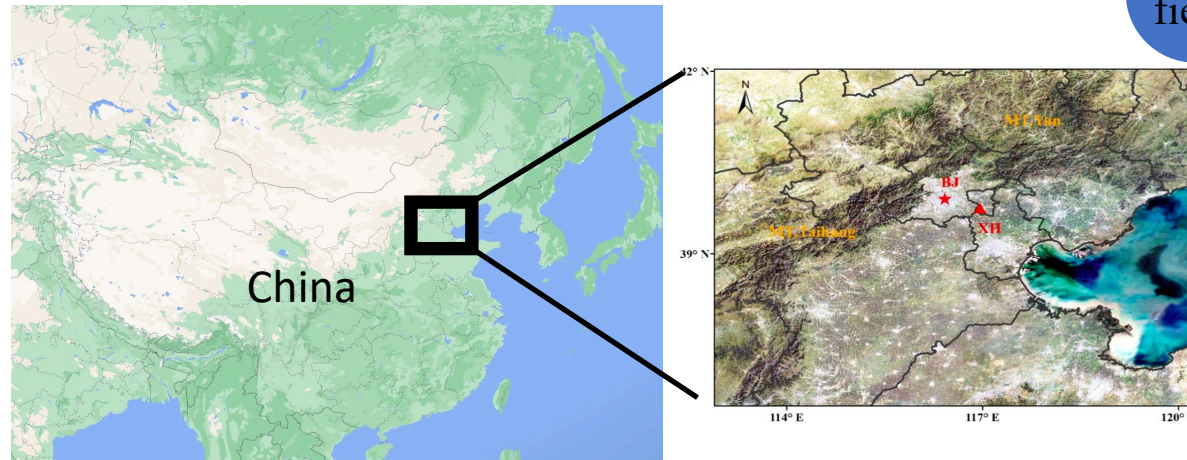
validation



gridded concentration and flux products

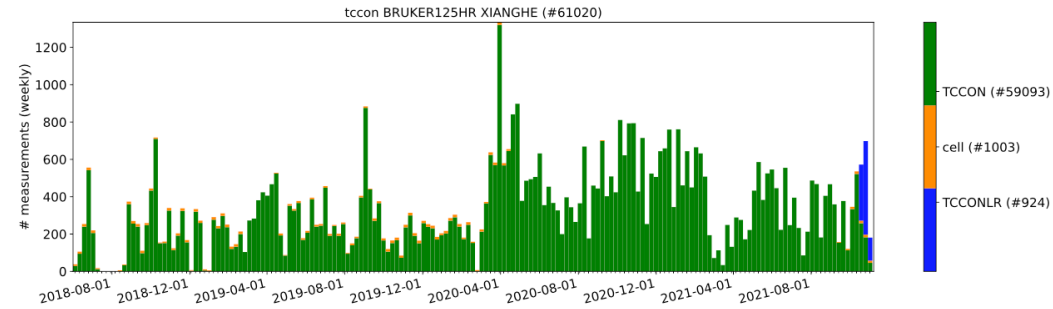
Instrument	Bruker 125HR	Bruker EM27/SUN
Location	Xianghe	Beijing Periphery
Observation mode	TCCON + partly NDACC (InSb)	COCCON
Operational state	normal	3 operational, 1 laboratory

Currently, one Bruker 125HR and four Bruker EM27/SUN spectrometers are available. Four EM27/SUN are mainly used for regional measurements in Beijing and surrounding areas and for organizing field observation experiments.



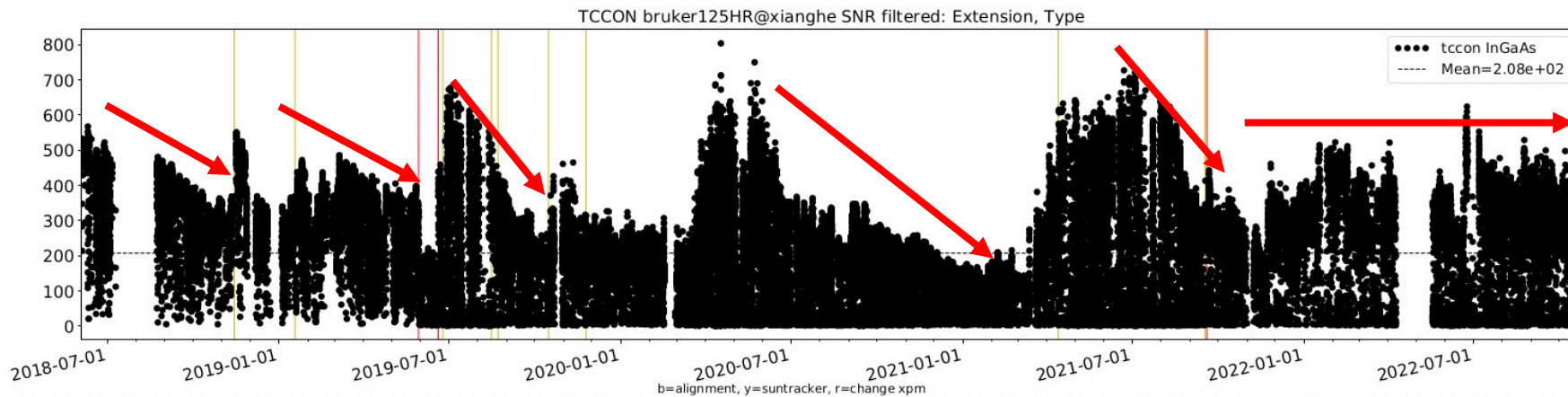


The number of observed spectra per week - 400

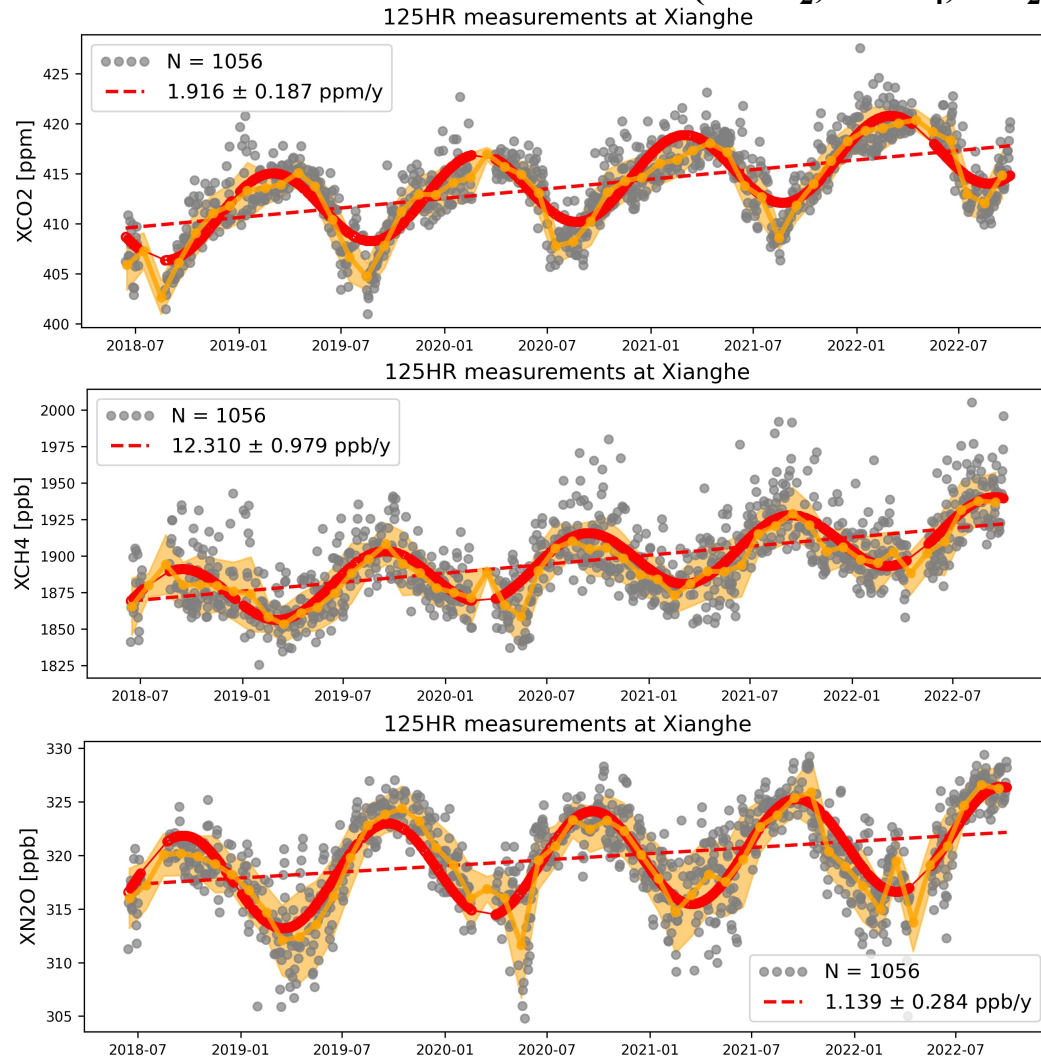


become a TCCON standard station in September 2021

- TCCON established harmonized standards for ground-based GHG remote sensing measurements (spectral signal-to-noise ratio, observation precision of meteorological parameters, retrieval algorithm, data quality control, etc.)



Time series of column-average dry-air mixing ratio of carbon dioxide, methane, and nitrous oxide (XCO₂, XCH₄, XN₂O)

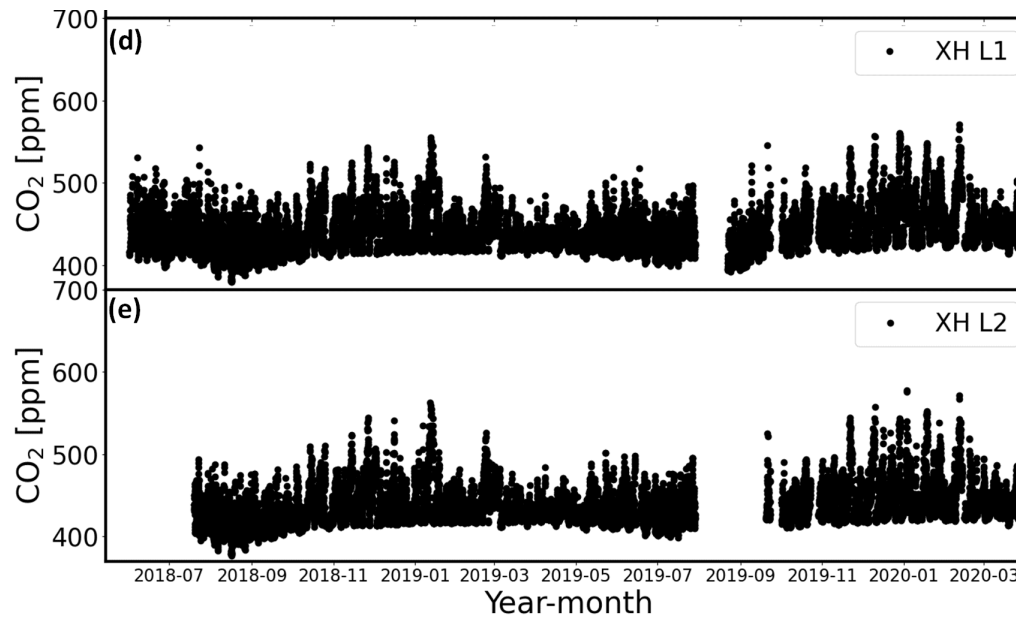
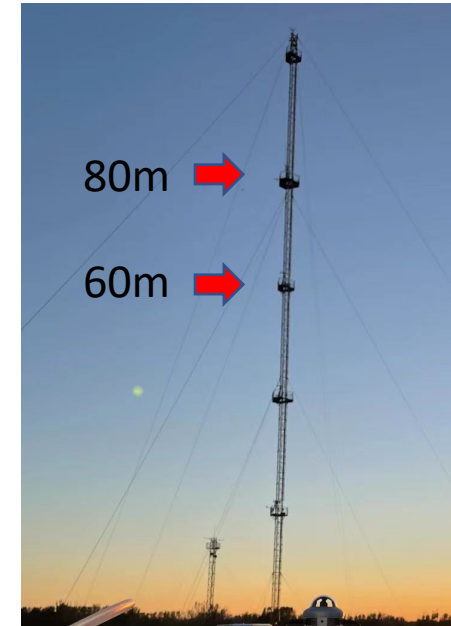
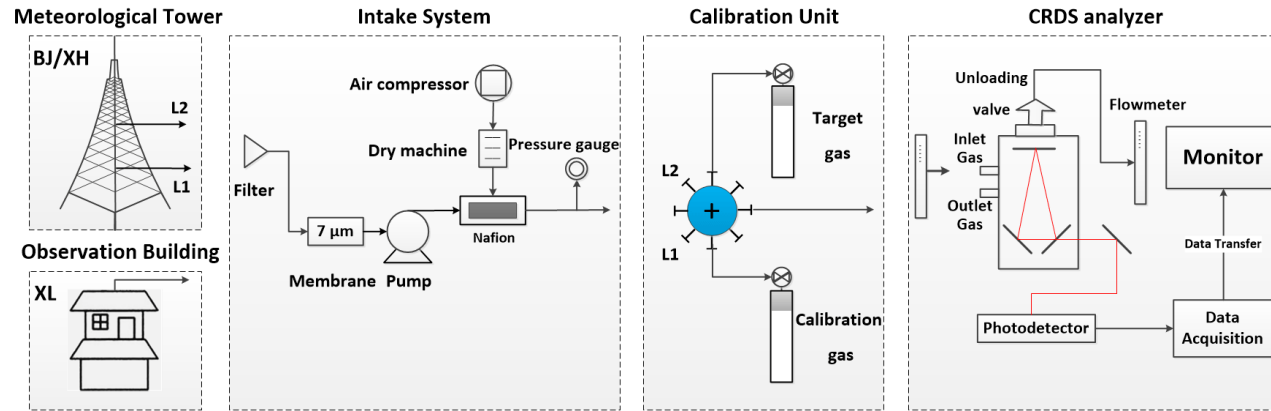


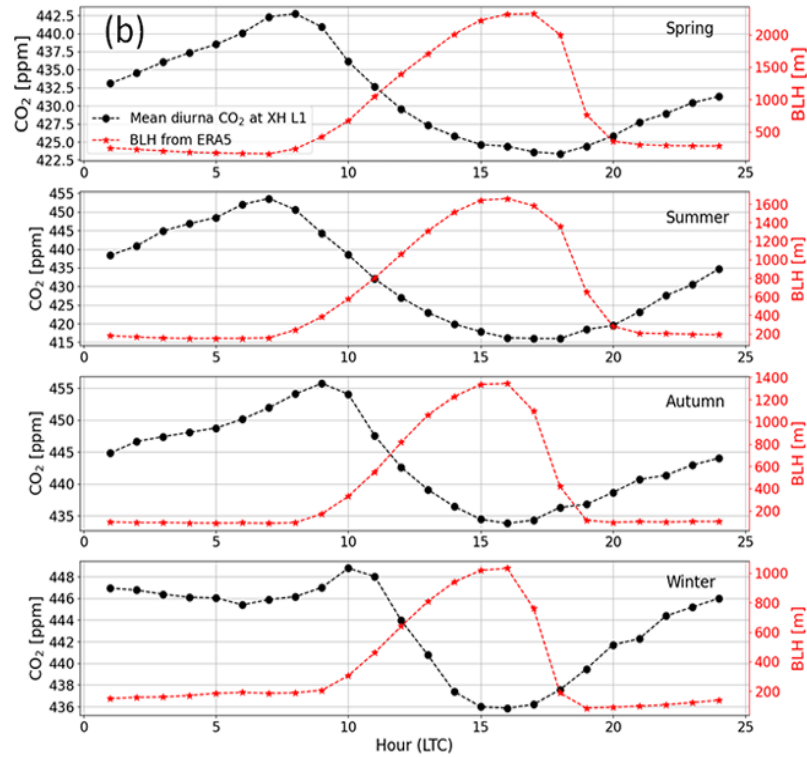
- The concentrations of XCO₂, XCH₄, XN₂O keep increasing.

	Xianghe TCCON	Mauna Loa
CO ₂	1.916ppm/year	2.38ppm/year
CH ₄	12.31ppb/year	14.37ppb/year
N ₂ O	1.139ppb/year	1.178ppb/year

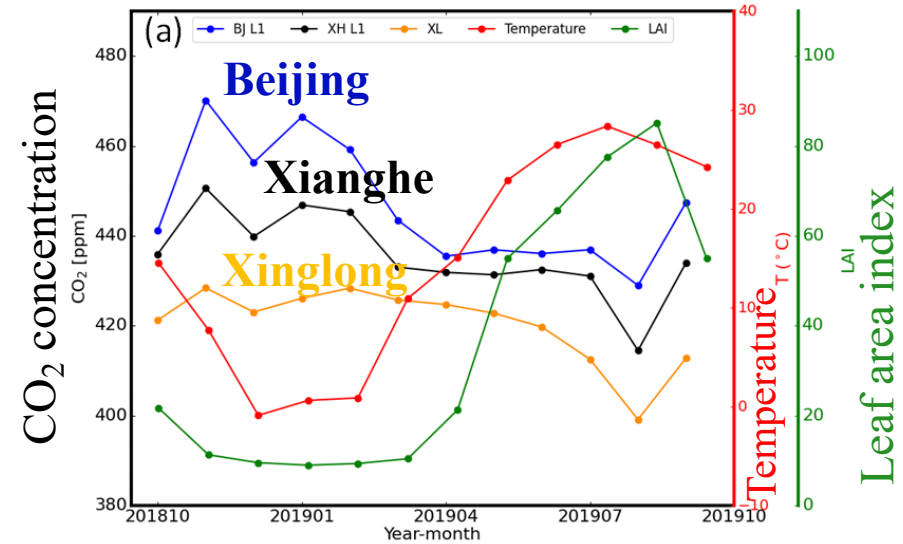
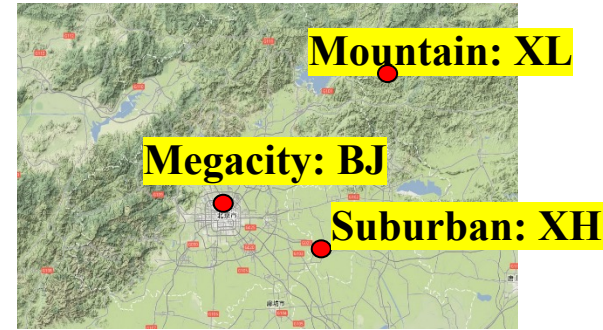
Yang, Zhou* et al., 2020 ESSD;
Zhou et al., 2022, RS
Zhou et al., in preparation

PICARRO observation system



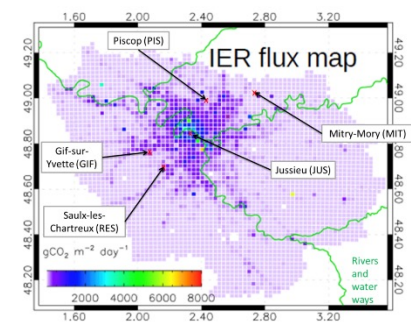
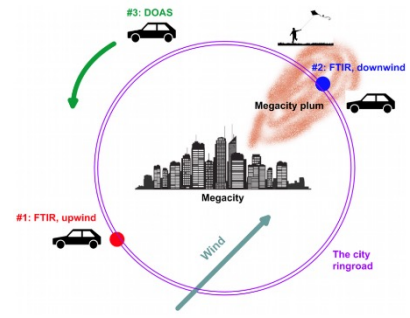
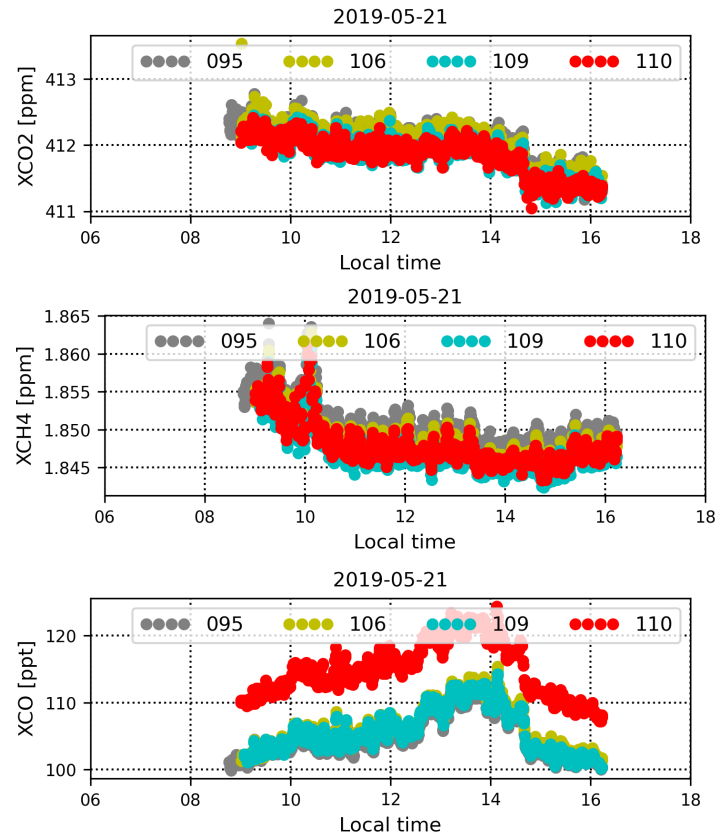


high at night and low at day;
associated with boundary layer changes



high in winter and low in summer;
associated with vegetation growth status

4 EM27/SUN (SN #095/#106/#109/#110) operated on the top floor of IAP-CAS

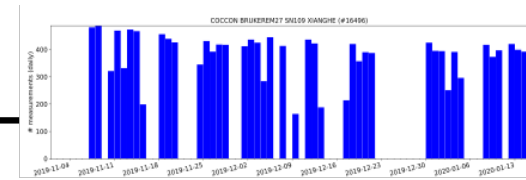


- ❖ There are discrepancies between EM27/SUN measurements, especially for XCO.
- ❖ Inter-instrument error should be corrected before organizing regional observation experiments.

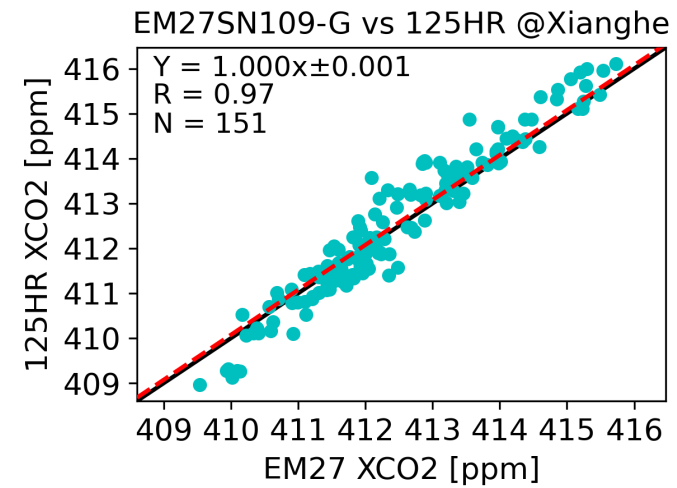
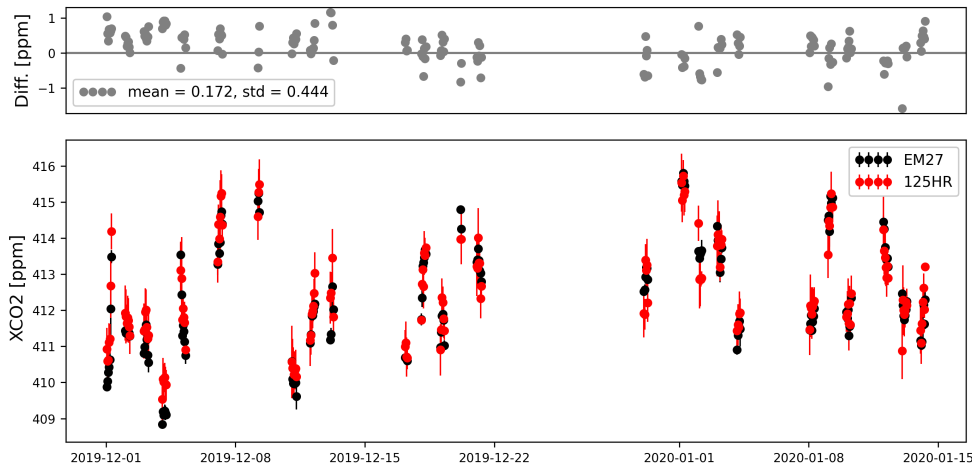
XCO₂, XCH₄, and XCO observed by four EM27/SUN measurements on 21 May 2019



Time line



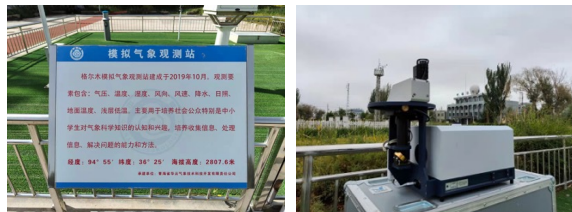
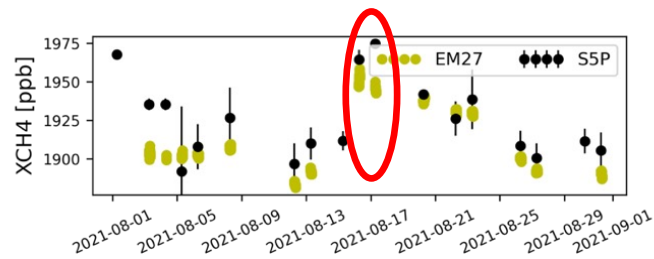
Bruker EM27/SUN SN109
201911 - 202001



❖ high correlation between EM27 and TCCON (R=0.97)

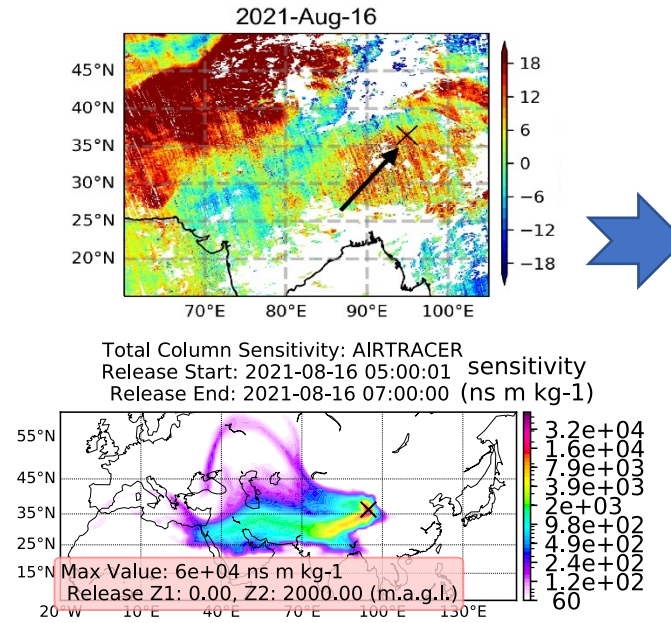
- In August 2021, the observation experiment of EM27/SUN at Golmud, Qinghai was organized;
- Aims of the experiment: validate satellite measurement errors; analyze variations of column concentrations of CO₂/CH₄/CO at Golmud

CH₄ high values observed in ground-based and satellite measurements



EM27/SUN GHG remote sensing observational experiment at Golmud

Analysis of the transport pathway of CH₄ high values



Combining remote sensing measurements and atmospheric transport models, the transport of CH₄ high values from India was observed in Qinghai.

Bruker 125HR FTIR



Pandora



Microwave CIMEL-318



Bruker EM27/SUN



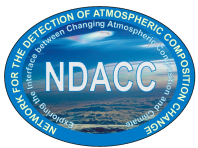
Brewer



MIN-DOAS MAX-DOAS

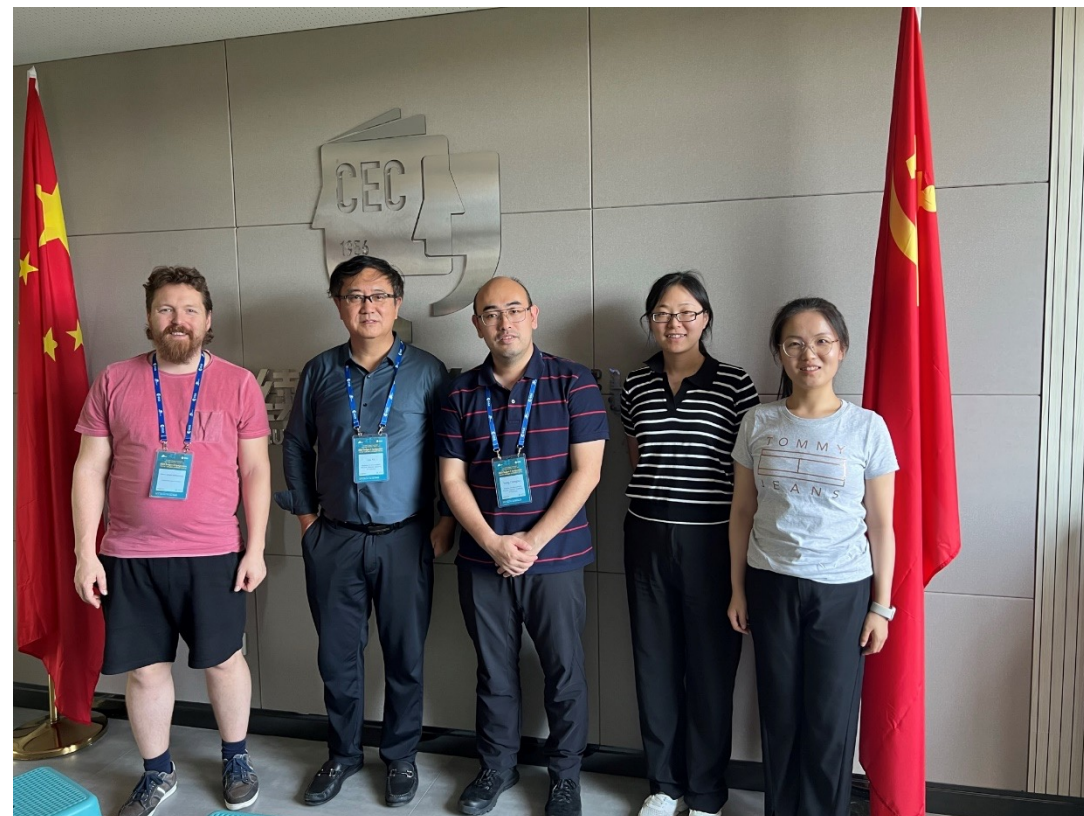


- Band: cover UV, VIS, IR
- pollutant gases, greenhouse gases, aerosols,
- near-surface, troposphere, stratosphere
- Strong international collaboration, e.g., TCCON, GAW, COCCON, AERONET...



ID. 59355

- Dr. Yang and Dr. Wang visiting University of Edinburgh (April- July 2023)
- Dr. Hakkarainen visiting Institute of Atmospheric Physics, CAS (Septemper 2023)
- Group meet at IMNU (Septemper 2023)



ID. 59355

TanSat city and hotspot emissions

TanSat coordinated with Sentinel-5P

COP27 video

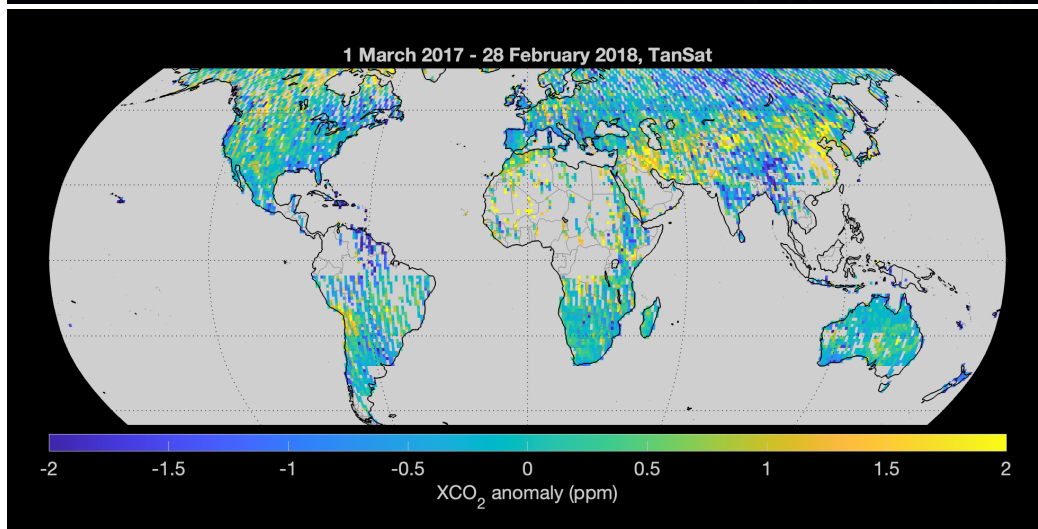
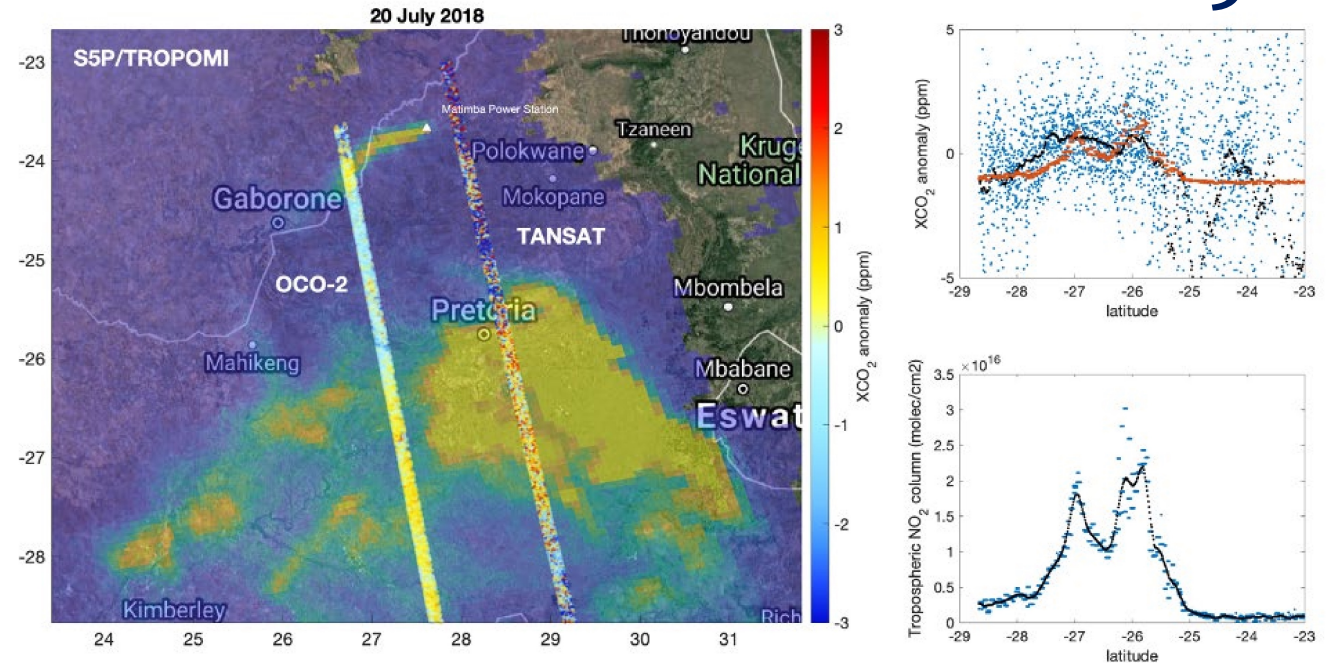
CHINESE TANSAT

ESA SENTINEL-5P

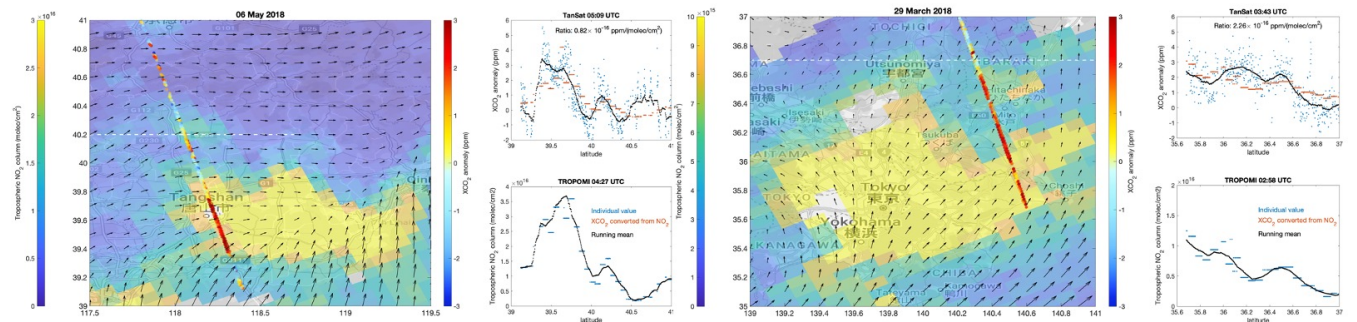
通过欧洲卫星和碳卫星分别监测到的数据
using data from both European satellite and TanSat

Detection of Anthropogenic CO₂ Emission Signatures with TanSat CO₂ and with Copernicus Sentinel-5 Precursor (S5P/NO₂) Measurements: First Results

中国科学院
CHINESE ACADEMY OF SCIENCES



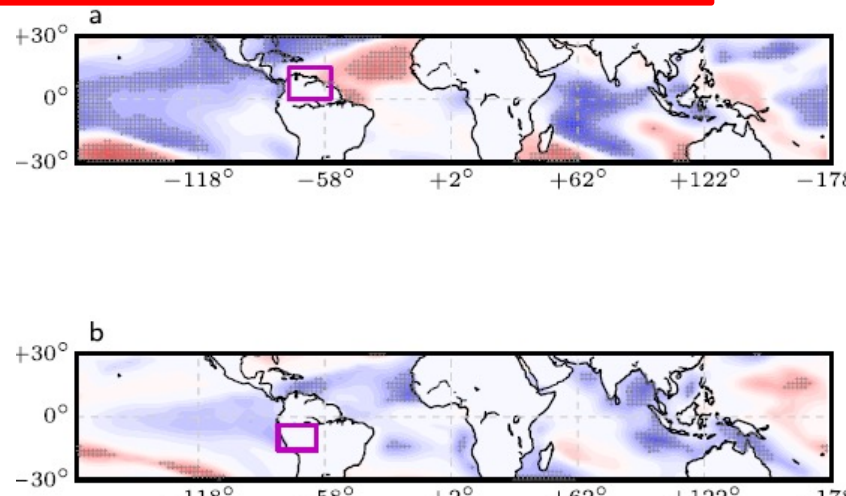
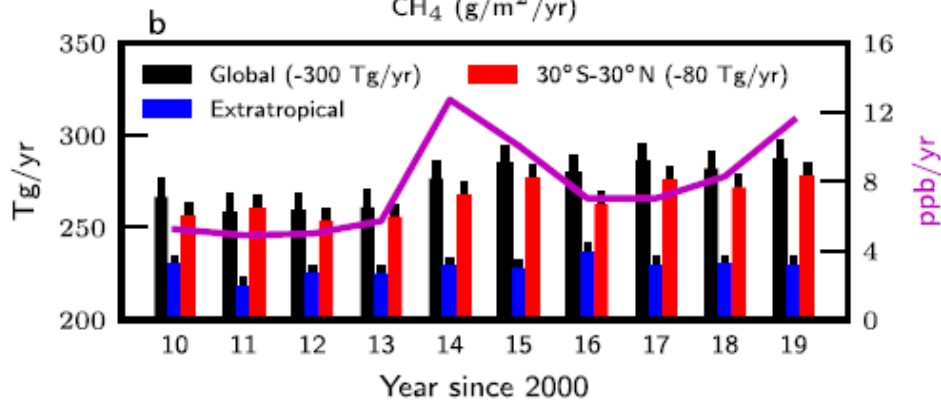
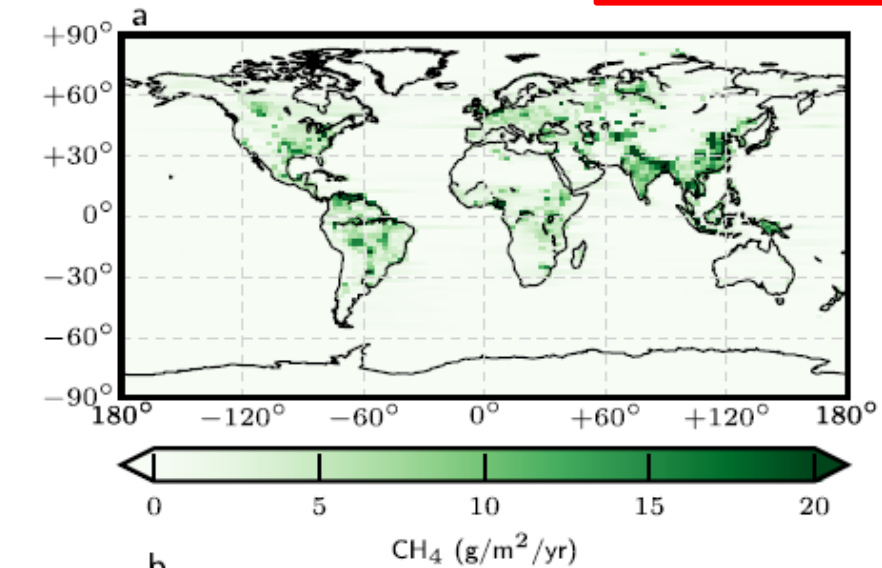
Yang D., Hakkarainen J., Liu Y., et al., 2023



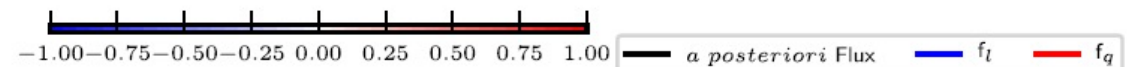
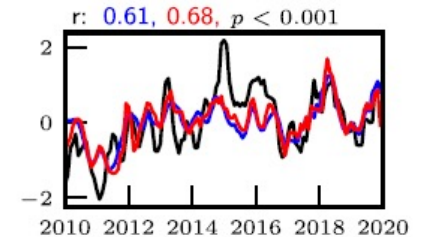
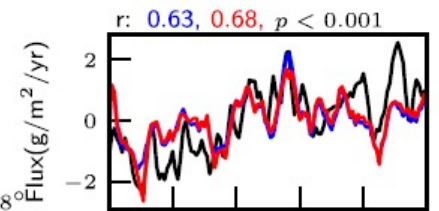
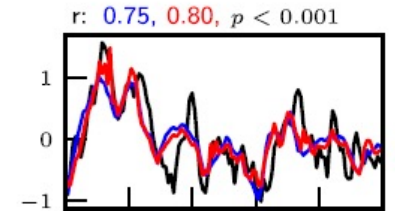
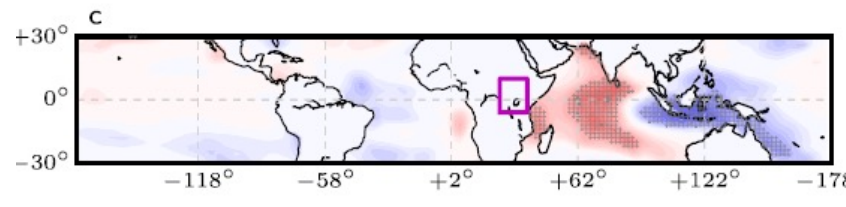
ID. 59355

- Tropical methane emissions, nearly 60% of global totals, explain 84% of global atmospheric methane growth rate
- **Sea surface temperature (SST)** variations could be used to help forecast variations in global atmospheric methane

Feng L., et al, 2022, Nature communication



SST— precipitation, surface temperature and soil moisture—tropical methane emissions

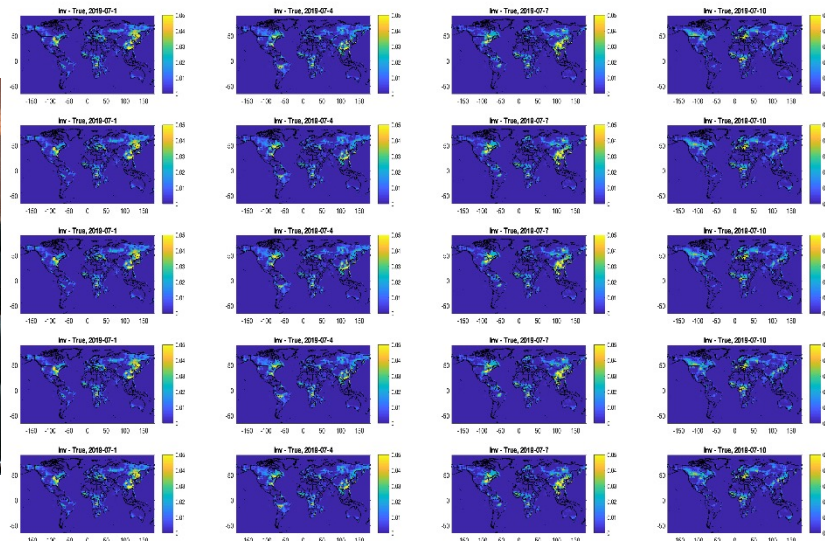


ID. 59355

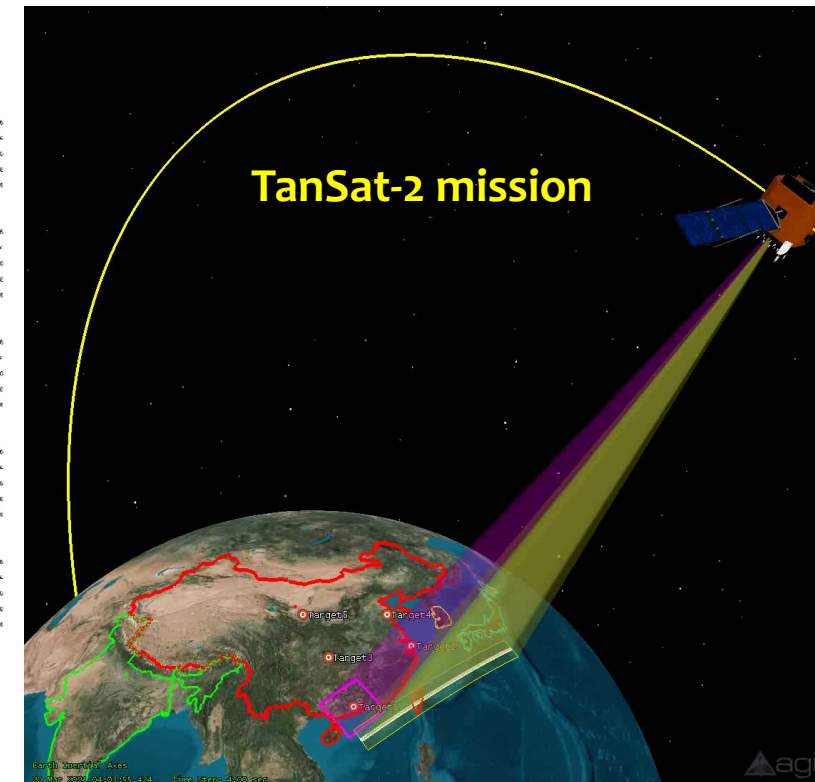
- TanSat-2 and CO2M cooperation and coordination in future
- New CO₂ and CH₄ retrieval algorithm development
- New methods for emission estimation from plume observation measurement
- Atmospheric inversion of CO₂ and CH₄ for contribute Global Stocktake



GHG MOST-ESA meeting



TanSat-2 OSSE and design





Dragon 5 3rd Year Results Reporting



Thank you!